

<sub>1</sub> Deep Underground Neutrino Experiment (DUNE)

<sub>2</sub> Technical Proposal

<sub>3</sub> **13 April 2018: Final draft of the TP volumes due**

<sub>4</sub> Volume 2: *The Single-Phase Far Detector*

<sub>5</sub> April 24, 2018



# **Contents**

<b>1</b>	<b>Contents</b>	<b>i</b>
<b>2</b>	<b>List of Figures</b>	<b>iii</b>
<b>3</b>	<b>List of Tables</b>	<b>iv</b>
<b>4</b>		
<b>5</b>	<b>1 Photon Detection System</b>	<b>1</b>
6	1.1 Photon Detection System (PDS) Overview . . . . .	1
7	1.1.1 Introduction . . . . .	1
8	1.1.2 Design Considerations . . . . .	2
9	1.1.3 Development and Evaluation Plans . . . . .	8
10	1.2 Photon Detector Efficiency Simulation . . . . .	9
11	1.3 Photon Detection System Design . . . . .	12
12	1.3.1 Photon Collector: ARAPUCA . . . . .	13
13	1.3.2 Photon Collector: Dip-Coated Light Guides . . . . .	18
14	1.3.3 Photon Collector: Double-Shift Light Guides . . . . .	19
15	1.3.4 Additional Techniques to Enhance Light Yield . . . . .	21
16	1.3.5 Silicon Photosensors . . . . .	22
17	1.3.6 Electronics . . . . .	25
18	1.4 Production and Assembly . . . . .	28
19	1.4.1 Photon Collector Production . . . . .	28
20	1.4.2 Photon Detector Module Assembly . . . . .	33
21	1.4.3 Incoming Materials Control . . . . .	33
22	1.4.4 Assembly Area Requirements . . . . .	33
23	1.4.5 Component Cleaning . . . . .	34
24	1.4.6 Assembly Procedures . . . . .	34
25	1.4.7 Post-Assembly Quality Control . . . . .	34
26	1.4.8 anode plane assembly (APA) Frame Mounting Structure and Module Securing .	35
27	1.4.9 Photosensor Modules . . . . .	37
28	1.4.10 Electronics . . . . .	38
29	1.5 System Interfaces . . . . .	39
30	1.5.1 Anode Plane Assembly . . . . .	40
31	1.5.2 Feedthroughs . . . . .	40
32	1.5.3 TPC Cold Electronics . . . . .	41
33	1.5.4 Cathode Plane Assembly and High Voltage System . . . . .	41
34	1.5.5 Data Acquisition . . . . .	42

1	1.5.6 Calibration and Monitoring . . . . .	43
2	1.6 Installation, Integration and Commissioning . . . . .	44
3	1.6.1 Transport and Handling . . . . .	44
4	1.6.2 Integration with APA and Installation . . . . .	45
5	1.6.3 Installation into the Cryostat and Cabling . . . . .	45
6	1.6.4 Commissioning - Calibration and Monitoring . . . . .	46
7	1.7 Quality Assurance and Quality Control . . . . .	46
8	1.7.1 Design Quality Assurance . . . . .	46
9	1.7.2 Production and Assembly Quality Assurance . . . . .	47
10	1.7.3 Production and Assembly Quality Control . . . . .	48
11	1.7.4 Installation Quality Control . . . . .	48
12	1.8 Safety . . . . .	49
13	1.9 Organization . . . . .	50
14	1.9.1 Single-Phase Photon Detection System Consortium Organization . . . . .	50
15	1.9.2 Planning Assumptions . . . . .	51
16	1.9.3 High-Level Schedule . . . . .	52
17	<b>References</b>	<b>55</b>
18		

# **List of Figures**

1.1	Schematic of scintillation light production in argon. . . . .	3
1.2	3D model of photon detectors in the APA. . . . .	5
1.3	Preliminary estimates of the efficiency for finding $t_0$ for SNB events. . . . .	11
1.4	Resolution on $t_0$ for supernova neutrino burst (SNB) events. . . . .	12
1.5	Schematic representation of the ARAPUCA operating principle. . . . .	14
1.6	ARAPUCA test at the Brazilian Synchrotron Light Laboratory. . . . .	15
1.7	Full-scale ARAPUCA for ProtoDUNE-SP during assembly. . . . .	16
1.8	ARAPUCA array in ProtoDUNE-SP. . . . .	17
1.9	X-ARAPUCA design: assembled cell (left), exploded view (right). . . . .	17
1.10	Schematic of scintillation light detection with dip-coated light guide bars. . . . .	18
1.11	Schematic of the principle of a double-shift light guide. . . . .	19
1.12	Predicted light yield with WLS-coated reflector foils on the cathode plane assembly (CPA). .	22
1.13	ProtoDUNE-SP Photon Detector readout. . . . .	26
1.14	ProtoDUNE-SP ARAPUCA modules during assembly. . . . .	29
1.15	ProtoDUNE-SP dip-coated light guide bars production. . . . .	30
1.16	Dip-coated acrylic plates. . . . .	31
1.17	EJ-280 light guide in darkbox for attenuation scan QA. . . . .	32
1.18	photon detector (PD) module scanner. . . . .	35
1.19	PD mounting rails in APA frame. . . . .	36
1.20	PD mechanical support analysis. . . . .	37
1.21	PDS consortium organization chart. . . . .	50
1.22	PDS consortium schedule through to the TDR. . . . .	52

# **List of Tables**

1.1	PDS performance requirements to achieve the primary science objectives. . . . .	2
1.2	Preliminary PD performance requirements. . . . .	3
1.3	Candidate photosensors characteristics. . . . .	24
1.4	Shrinkage of PD materials. . . . .	35
1.5	Relative shrinkage of PD components and APA frame with mitigations . . . . .	36
1.6	Pre-Technical Design Report Key Milestones. . . . .	53
1.7	Post-Technical Design Report Key Milestones. . . . .	53

9

# **1 Todo list**

<sup>2</sup> All done, no? . . . . .	9
<sup>3</sup> full detector or SP module? . . . . .	10
<sup>4</sup> want to specify Brazil? . . . . .	28

# <sup>1</sup> Chapter 1

## <sup>2</sup> Photon Detection System

### <sup>3</sup> 1.1 Photon Detection System (PDS) Overview

#### <sup>4</sup> 1.1.1 Introduction

<sup>5</sup> The photon detection system (PDS) is an essential subsystem of a DUNE SP module. The detec-  
<sup>6</sup> tion of the prompt scintillation light signal, emitted in coincidence with an ionizing event inside  
<sup>7</sup> the active volume, allows the determination of the time of occurrence of an event of interest with  
<sup>8</sup> much higher precision than charge collected from ionization in the TPC. This capability is most  
<sup>9</sup> critical for the primary DUNE science objectives that are uncorrelated with the timing signal from  
<sup>10</sup> the neutrino source at Fermilab, such as proton decay and neutrinos from a SNB, and for the ancil-  
<sup>11</sup> lary science program including measurements of neutrino oscillation phenomena using atmospheric  
<sup>12</sup> neutrinos.

<sup>13</sup> Timing information from the PD and TPC systems allows determination of the drift time of the  
<sup>14</sup> ionizing particles. Knowledge of the drift time provides localization of the event inside the active  
<sup>15</sup> volume and provides the ability to correct the measured charge for effects that depend on the drift  
<sup>16</sup> path length, purity of LAr, or for specific locations in the detector if there are non-uniformities.  
<sup>17</sup> This correction is important for the reconstruction of the energy deposited by the ionizing event.  
<sup>18</sup> In addition to allowing optimum track reconstruction, scintillation light measured by the system  
<sup>19</sup> may also be used as a trigger and for improved calorimetric measurement in combination with  
<sup>20</sup> charge measurement.

<sup>21</sup> [tab:pds-sys-req](#) Table 1.1 summarizes the high-level system performance requirements for the PDS necessary to  
<sup>22</sup> achieve the DUNE science objectives. The first row provides a requirement to ensure high effi-  
<sup>23</sup> ciency and good energy resolution for proton decay and atmospheric neutrinos. The second row  
<sup>24</sup> targets core collapse SNB neutrinos, but specifies only a timing measurement for event localization  
<sup>25</sup> (in conjunction with the TPC drift time measurement). However, a consensus has emerged in the  
<sup>26</sup> collaboration that the current requirements do not fully exploit the potential for LAr scintillation  
<sup>27</sup> light to contribute to the energy reconstruction of events, in particular for lower energy events

- <sup>1</sup> such as from SNBs (10-100 MeV). In response, the third row is a proposed requirement to measure  
<sup>2</sup> the energy in scintillation light from SNB events near the peak of the spectrum ( $\sim 10$  MeV) with a  
<sup>3</sup> precision similar to that of the ionization measurement. The combined measurement of ionization  
<sup>4</sup> charge and scintillation light has been shown to improve the determination of the energy depo-  
<sup>5</sup> sition of an event. Table 1.2 shows the corresponding photon detection light yield, timing and  
<sup>6</sup> spatial separation requirements. To achieve a 10% calorimetric measurement with light requires  
<sup>7</sup> approximately ten times higher light yield for the PDS than the original requirement.
- <sup>8</sup> To achieve these requirements, there is an ongoing intense R&D program to investigate methods  
<sup>9</sup> that maximize the photon detection efficiency of the PDS within the constraints of the SP TPC  
<sup>10</sup> design . All three of the photon collector options described in this chapter could meet the original  
<sup>11</sup> performance requirements, albeit with different event efficiency, but one, the ARAPUCA, has  
<sup>12</sup> highest potential to perform the low energy calorimetric measurements at the desired precision. It  
<sup>13</sup> also has the highest efficiency for SNB events and provides higher spatial granularity for background  
<sup>14</sup> rejection.

Table 1.1: PDS performance requirements to achieve the primary science objectives (under review).

Requirement	Rationale
The far detector (FD) PDS shall detect sufficient light from events depositing visible energy $> 200$ MeV to efficiently measure the time and total intensity.	This is the region for nucleon decay and atmospheric neutrinos. The time measurement is needed for event localization for optimal energy resolution and background rejection.
The FD PDS shall detect sufficient light from events depositing visible energy $< 200$ MeV to provide a time measurement. The efficiency of this measurement shall be adequate for SNB events.	Enables low energy measurement of event localization for SNB events. The efficiency may vary significantly for visible energy in the range 5 MeV to 100 MeV.
(Proposed) The FD PDS shall detect sufficient light from events depositing visible energy of 10 MeV to provide an energy measurement with a resolution of 10%.	Enables energy measurement for SNB events with a precision similar to that from the TPC ionization measurement.
The FD PDS readout electronics shall record time and signal amplitude from the photo-sensors with sufficient precision and range to achieve the key physics parameters.	The resolution and dynamic range needs to be adjusted so that a few-photoelectron signal can be detected with low noise. The dynamic range needs to be sufficiently high to measure light from a muon traversing a TPC module.

### <sup>15</sup> 1.1.2 Design Considerations

<sup>16</sup> *Scintillation Light:* Liquid argon (LAr) is known to be an abundant scintillator and emits about  
<sup>17</sup> 40 photons/keV when excited by minimum ionizing particles<sup>[?]</sup>, in the absence of external E fields.  
<sup>18</sup> In the presence of E fields the yield is reduced due to recombination; for the nominal DUNE SP  
<sup>19</sup> module field of 500 V/cm the yield is approximately 24 photons/keV <sup>[?]</sup>.

Table 1.2: Photon detector performance requirements (under review).

Parameter	Value
(Current) Minimum detector response per MeV energy deposition (Light Yield).	1 pe/MeV for events at the center of the TPC and no less than 0.5 pe/MeV at all points in the fiducial volume.
(Proposed) Minimum detector response per MeV energy deposition (Light Yield).	10 pe/MeV for events at the center of the TPC and no less than 5 pe/MeV at all points in the fiducial volume.
Minimum requirements on energy deposition, spatial separation, and temporal separation from other events, for which the system must associate a unique event time ( <i>flash matching</i> ). det-req	10 MeV, 1 m, 1 ms respectively.

As depicted in Figure 1.1, the passage of ionizing radiation in LAr produces excitations and ionization of the argon atoms that ultimately results in the formation of the excited dimer  $\text{Ar}_2^*$ . Photon emission proceeds through the de-excitation of the lowest lying singlet and triplet excited states,  ${}^1\Sigma$  and  ${}^3\Sigma$  to the dissociative ground state. The de-excitation from the  ${}^1\Sigma$  state is very fast and has a characteristic time of the order of  $\tau_{fast} \simeq 6\text{ ns}$ . The de-excitation from the  ${}^3\Sigma$  state is much slower with a characteristic time of  $\tau_{slow} \simeq 1.3\text{ }\mu\text{sec}$ , since it is forbidden by the selection rules. In both decays, photons are emitted in a 10 nm band centered around 128 nm, which is in the Vacuum Ultra-Violet (VUV) region of the electromagnetic spectrum. The relative intensity of the fast and slow components is related to the ionization density of LAr and depends on the ionizing particle: 0.3 for electrons, 1.3 for alpha particles and 3 for neutrons [?]. This phenomenon is the basis for the particle discrimination capabilities of LAr exploited by many experiments that have the capacity to separate the two components, for DUNE the greatest significance relates to a pending decision on treatment of light signals.

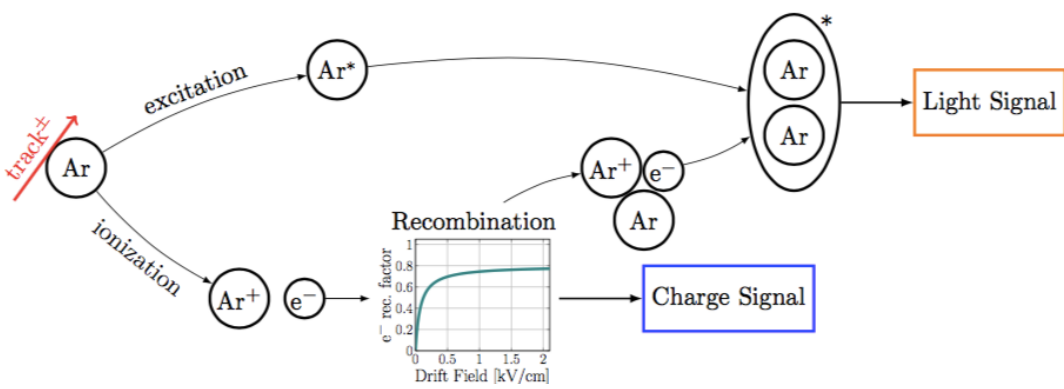


Figure 1.1: Schematic of scintillation light production in argon.

In massive LArTPCs, a cost-effective approach is to use photon collector systems that collect light from large areas and attempt channel it in an efficient way towards much smaller photosensors that produce an electrical signal. This paradigm for the detection of LAr scintillation light depends on the use of chemical wavelength shifters since most currently available commercial (cryogenic) large area photosensors are not directly sensitive to VUV radiation, primarily due to the lack of

<sup>1</sup> transparency of fused silica and glass optical windows.

<sup>2</sup> <sup>39</sup>Ar: The long-lived cosmogenic radioisotope <sup>39</sup>Ar has a natural abundance with an activity  
<sup>3</sup> of approximately 1 Bq/kg and undergoes beta decay with a mean beta energy of 220 keV with  
<sup>4</sup> an endpoint of 565 keV. In the 10 kt FD modules this leads to a rate of more than 10 MHz of  
<sup>5</sup> very short ( $\sim$ 1 mm) tracks uniformly distributed throughout the detector module, each of which  
<sup>6</sup> produces several thousand VUV scintillation photons. This continuous background impacts the  
<sup>7</sup> data aquisition (DAQ), trigger and spatial granularity required of the PDS.

<sup>8</sup> *Wavelength Shifter*: The most widely used wavelength shifter used in combination with LAr is  
<sup>9</sup> Tetra-Phenyl Butadiene (TPB)<sup>1</sup>, which absorbs VUV photons and re-emits them with a spec-  
<sup>10</sup> trum centered around 420 nm, close to where most commercial photosensors have their maximum  
<sup>11</sup> quantum efficiency for photoconversion. Though TPB has been studied quite extensively with  
<sup>12</sup> great success, there are recent publications that warrant caution. For example, until recently the  
<sup>13</sup> conversion efficiency of TPB in coating was taken to be high, approaching or even exceeding 100%  
<sup>14</sup> (possible by multi-photon emission), however a recent arXiv paper [?] refutes this previous fre-  
<sup>15</sup> quently referenced result. Using much of the same equipment but replacing a damaged reference  
<sup>16</sup> photodiode, the authors (including an author of the previous paper) report a measurement for the  
<sup>17</sup> quantum efficiency of 40% for incident 128 nm light. Another recent paper[?] reports that some  
<sup>18</sup> methods used to coat surfaces with TPB suffered loss of the TPB coating in LAr, whereas there  
<sup>19</sup> is no measurable effect if the fluor is dissolved in a polymer matrix. These developments will be  
<sup>20</sup> followed carefully and highlight the importance of the ongoing R&D and prototype program.

<sup>21</sup> *Physical Constraints*: The physical dimension of the PD system is constrained by the need to fit  
<sup>22</sup> within the innermost wire planes of the anode plane assemblies and to be installed through slots  
<sup>23</sup> in the APA mechanical frame after it is wound (see Section ??). Individual PD modules will be  
<sup>24</sup> restricted to be within an envelope in the form of a long, thin box. At the time of preparation of  
<sup>25</sup> this proposal the dimensions were 14.6 cm  $\times$  9.6 cm  $\times$  212.7 cm, but it is anticipated that the size  
<sup>26</sup> of the slot in the APA will be increased by about 25% (the long dimension of the modules will  
<sup>27</sup> remain the same). There will be ten PD modules per APA, for a total of 1500 modules.

### <sup>28</sup> 1.1.2.1 Photon Collectors

<sup>29</sup> The core modular elements of the PDS are the large area *photon collectors* that convert inci-  
<sup>30</sup> dent 128 nm scintillation photons into photons in the visible range ( $>400$  nm), which in turn are  
<sup>31</sup> converted to an electrical signal by compact (silicon photomultipliers (SiPMs)). As detailed in  
<sup>32</sup> Section I.3, since the size and cost of currently available SiPMs are not well matched to meeting  
<sup>33</sup> the performance requirements in the large-volume SP module, the photon collector design aims to  
<sup>34</sup> maximize the active VUV-sensitive area of the PD module while minimizing the necessary photo-  
<sup>35</sup> cathode (SiPM) coverage. In the following we will distinguish between the terms *photon collection*  
<sup>36</sup> efficiency and *photon detection* efficiency. Collection efficiency is the number of visible photons  
<sup>37</sup> delivered to the SiPMs divided by the number of VUV photons incident on the PD module active  
<sup>38</sup> area; this parameter is used to report results of calculations or simulations of predicted device  
<sup>39</sup> performance independent of the SiPM used. Detection efficiency is the number of detected ph-

<sup>1</sup>1,1,4,4-Tetraphenyl-1,3-butadiene, supplier: Sigma-Aldrich®.

<sup>1</sup> to electron from the SiPM(s) divided by the number of VUV photons incident on the PD module  
<sup>2</sup> active area; this is generally the result of a direct measurement unless the detailed performance of  
<sup>3</sup> the SiPM is known and divided out. The *effective area* of a PD module is another useful figure-  
<sup>4</sup> of-merit that is defined to be the photon detection efficiency multiplied by the photon collecting  
<sup>5</sup> area of a PD module.

<sup>6</sup> Three different designs of PD photon collector modules have been developed and are being con-  
<sup>7</sup> sidered by the SP PD consortium. The baseline design, ARAPUCA<sup>2</sup>, is a relatively new concept  
<sup>8</sup> that is scalable and has the potential for the best performance of the three designs by a signifi-  
<sup>9</sup> cant factor. It is functionally a light trap that captures wavelength-shifted photons inside boxes  
<sup>10</sup> with highly reflective internal surfaces where they are eventually detected by SiPMs. There are  
<sup>11</sup> also two alternative designs based on the use of wavelength-shifters and light guides coupled to  
<sup>12</sup> SiPMs. Both have undergone more development than ARAPUCA but their performance meets  
<sup>13</sup> the basic physics requirements with only a limited safety margin and are not easily scalable within  
<sup>14</sup> the geometric constraints of the SP module. Figure 1.2 shows a 3D model of the SP TPC with a  
<sup>15</sup> zoom in to the anode plane where the three candidates photon collector technologies are visible  
<sup>16</sup> for illustration – in the final detector module there will be a single type.



Figure 1.2: 3D model of photon detectors in the APA. The model on the left shows the full width of the TPC with the configuration APA-CPA-APA-CPA-APA. The figure on the right shows a zoom in to the top far side of the TPC where three candidates photon collector technologies are visible for illustration - in the final detector there will be a single type.

<sup>17</sup> **ARAPUCA Option:** The first large-scale implementation of an ARAPUCA module, in ProtoDUNE-  
<sup>18</sup> SP, is composed of an array of sixteen ARAPUCA cells each one acting as an individual detector  
<sup>19</sup> element. This configuration allows for finer spatial segmentation along the detector bar than is the  
<sup>20</sup> case for the light guide designs. The ProtoDUNE-SP ARAPUCA design collects light from one  
<sup>21</sup> side of the box through an optical window formed by a dichroic filter deposited with a layer of pTP<sup>3</sup>  
<sup>22</sup> wavelength shifter on the external surface. This shifts the incident VUV light to a near-visible  
<sup>23</sup> frequency that is able to pass through the filter plate to the interior of the box.

<sup>24</sup> In the ProtoDUNE-SP version of the device, the inner surface of the box opposite the window

<sup>2</sup>Arapuca is the name of a simple trap for catching birds originally used by the Guarani people of Brazil.

<sup>3</sup>p-TerPhenyl, supplier: Sigma-Aldrich®.

fig:3dtpc\_pd

1 houses an array of SiPMs that covers a small fraction of the area of the window (2.8-5.6%),  
2 surrounded by a foil of a highly reflective material coated with a second wavelength shifter, TPB.  
3 The TPB converts the light passing through the filter to a wavelength that will be reflected by  
4 the filter. It has been shown in simulation and in prototypes that a large fraction of these trapped  
5 photons, reflecting from the filter and the lined walls of the box, will eventually fall on a SiPM and  
6 be detected. The X-ARAPUCA described in Section 1.3.1.3, is a promising variant of the concept  
7 that uses a wavelength shifter-doped plate between two dichroic filter windows with SiPMs on the  
8 narrow sides of the cell; in addition to viewing scintillation light from both sides as needed for the  
9 central APA, it is expected to provide a higher light collection efficiency.

10 The ARAPUCA concept is relatively recent – it was first proposed in 2015 and accepted for  
11 installation in ProtoDUNE-SP in mid-2016. A series of tests in LAr have been performed with an  
12 evolving prototype design that resulted in detection efficiency measurements ranging from 0.4%  
13 to 1.8%, demonstrating the potential for substantially higher performance than the light guide  
14 designs. Monte Carlo (MC) simulations show that detection efficiencies at the level of several per  
15 cent could be reasonably reached with improvements to the basic design. While the results of the  
16 experimental tests are encouraging, a deeper understanding of the optical phenomena involving  
17 emission and scattering on wavelength-shifter coated surfaces is needed to optimize the design.

18 **Light Guide Options:** The fundamental idea of this approach is to convert VUV scintillation light  
19 to visible wavelengths on (or near) the surface of an optical light guide, which then guides some  
20 fraction of the converted light by total internal reflection to SiPMs mounted on one or both ends  
21 of the guide.

22 Several approaches were investigated and narrowed down to the two most promising ones based a  
23 set of comparative measurements taken simultaneously in LAr [?]. These two have been improved  
24 over several years and have reached a reasonable level of maturity and reliability. The *dip-coated*  
25 light guides are pre-treated commercially-cut acrylic bars that are dip-coated with a solution of  
26 TPB, acrylic, and toluene. When the toluene evaporates it leaves a thin film of TPB embedded  
27 in the acrylic matrix on the surface of the bar. In the *double-shift* light guides, the conversion and  
28 guiding processes of the photons are decoupled. The first conversion is in a *radiator plate*, which is  
29 an ultraviolet transmitting UVT-acrylic plate coated with pure TPB through a spraying process.  
30 It is positioned just above a commercial WLS-doped bar that absorbs the blue light produced by  
31 TPB and re-emits it in the green; a fraction of this green light propagates down the bar.

32 Both bar designs have demonstrated attenuation lengths for the trapped light along the long  
33 dimension of the bar comparable to the length of the bars themselves, which ensures a reasonable  
34 uniformity along the beam direction. Preliminary measurements of both designs with readout  
35 at just one end indicate an photon detection efficiency range of 0.1% to 0.25% averaged along  
36 the length of the bar. Up to a factor of four higher detection efficiency might be achieved with  
37 straightforward enhancements, such as: SiPM at both ends of the bars; higher PDE SiPM; and  
38 coating the long edges of the bars with reflective foils.

### **1.1.2.2 Wavelength Shifter-Coated Cathode Plane**

Since the PD modules are installed only on the anode plane, light collection is not uniform over the entire active volume of the TPC. A possible solution to improve this is to install a reflective foil coated with wavelength shifter on the cathode. This would increase the light yield of the detector and could enable calorimetric measurements based on light emitted by the ionizing particles. It may also be possible to remove the  $^{39}\text{Ar}$  background through PD-supplied timing cuts, a background that may otherwise cause a huge counting rate for events near the anode plane. This option would require good visible light sensitivity for the photon collectors, which is not the case for current light collector options. The capability could be incorporated in a variety of ways but with an impact on the direct light measurement. This option has yet to be formally adopted by the PD consortium but is under study through MC simulations and the mechanical feasibility is being discussed with the high voltage (HV) consortium.

### **1.1.2.3 Silicon Photosensors**

In each photon collector concept, the final stage of converting a visible wavelength photon into an electrical signal is performed by a SiPM. The device must operate reliably for many years at LAr temperatures. Our experience with a promising early candidate that failed in later batches, due to an unadvertised change in the fabrication process, has emphasized the importance of a multi-source approach where we are actively engaged with potential vendors to develop a device expressly for cryogenic operation. Currently, there are ongoing investigations of MPPCs (Multi-Pixel Photon Counter) produced by Hamamatsu (Japan) including a model specifically designed for cryogenic operation, and a device developed for operation in LAr by FBK (Fondazione Bruno Kessler, Italy) in collaboration with the DarkSide experiment.

### **1.1.2.4 Readout Electronics**

For prototype development and for ProtoDUNE-SP, a waveform digitizer has been developed that enables a thorough investigation of the photosensor signals, particularly as we investigate the impact of electrically ganging multiple SiPMs. The design of the readout electronics for the final system will be strongly influenced by the outcomes of MC simulations that are in progress. Of particular interest is the extent to which pulse shape capabilities are important to maximizing sensitivity to low energy neutrino interactions from SNBs. Initial MC simulations suggest that it may not be necessary to fully digitize the SiPM waveforms in order to achieve the PD performance requirements. Charge integration electronic readout systems, which offer the promise of significantly lower cost and smaller cabling harnesses, are under investigation and are expected to be the baseline solution. A lower-cost waveform digitization based on lower sampling rate commercial electronics will be investigated as a potential backup option in case our evolving understanding of the requirements necessitates collecting waveform data from the SiPMs.

The size of currently available SiPMs is far smaller than the spatial granularity required for the experiment so the output of individual devices will be electrically summed (ganged) to reduce the

1 electronics channel count. This will be achieved either by simply connecting together the output  
2 of multiple devices, *passive ganging*, or using active components, *active ganging*, if the signal is  
3 too degraded. Both approaches are under investigation.

#### 4 **1.1.2.5 R&D Priorities**

5 Since the light guide designs are comparatively well understood, the need for an improved un-  
6 derstanding of the potential ARAPUCA performance drives the strategy for the R&D program  
7 that will be carried out before the Technical Design Report (TDR) (mid-2019). An intense effort  
8 is underway to demonstrate that an implementation of the ARAPUCA concept will increase the  
9 light yield of the SP module by a factor of five to ten with respect to the light guides; resources  
10 (personnel and funding) are being sought by the consortium to achieve this. Since the ARAPUCA  
11 approach demands a larger number of SiPMs than the light guides, a related high priority is  
12 demonstration of active ganging of a sufficient number of devices with adequate S/N properties.

13 It is anticipated that by the time of the TDR, the consortium will present ARAPUCA as a baseline  
14 design for the photon collector with one alternative design for risk mitigation.

#### 15 **1.1.3 Development and Evaluation Plans**

16 The performance of the different photon collection options will be evaluated at several facilities  
17 available to the consortium. Relative and absolute measurements will be performed at both room  
18 and cryogenic temperatures.

19 The most comprehensive set of data will come from the fully instrumented modules in the ProtoDUNE-  
20 SP experiment currently under construction at CERN, which will start operations in the last third  
21 of 2018. All three photon collector designs are present in ProtoDUNE-SP: 29 double-shift guides,  
22 29 dip-coated guides, and two ARAPUCA arrays. The TPC will provide precise reconstruction in  
23 3D of the track of any ionizing event inside the active volume and matching the track with the as-  
24 sociated light signal will enable an accurate comparison of the relative detection efficiencies of the  
25 different PD modules. In principle, absolute measurements are possible using MC simulations, but  
26 currently some of the optical parameters that regulate VUV light propagation in LAr are poorly  
27 known, which will limit the precision of the absolute measurements. A plan will be developed to  
28 address this limitation.

29 ProtoDUNE-SP will also provide a long-term test of full-scale PD modules for the first time so  
30 it may be possible to quantify any deterioration in their performance such as the loss of TPB  
31 from the coating noted previously. More broadly, aging effects in various detectors technologies,  
32 such as scintillator and photomultiplier tubes (PMTs), are well documented and knowledge of such  
33 effects is required at the design stage so that the photon detection performance will meet minimum  
34 requirements for the whole life of the experiment.

35 An R&D program will be executed in parallel with the ProtoDUNE-SP operation since additional

- <sup>1</sup> comparative measurements will be needed, particularly for the newer ARAPUCA concept, prior  
<sup>2</sup> to establishing the baseline design for the TDR. Several facilities are accessible to the consortium  
<sup>3</sup> that will allow testing of smaller scale prototypes of the modules (or sections of them). These  
<sup>4</sup> include: the cryogenic facilities at Fermilab, Colorado State University and Universidade Estadual  
<sup>5</sup> de Campinas (UNICAMP); and facilities for precision optical measurements and cryogenic testing  
<sup>6</sup> of photosensors at Fermilab, Indiana University, Northern Illinois University, University of Iowa,  
<sup>7</sup> Syracuse University, UNICAMP, and Institute of Physics in Prague.
- <sup>8</sup> A critical issue for large experiments are the interfaces between the subsystems. PD modules and  
<sup>9</sup> interfaces with the APA system and cold electronics will be conducted using cryogenic gaseous  
<sup>10</sup> nitrogen in cold box studies at CERN, using a test stand developed for testing of ProtoDUNE-SP  
<sup>11</sup> components prior to installation into the detector. A full-scale ProtoDUNE-SP APA is currently  
<sup>12</sup> being fabricated,

<sup>13</sup> All done, no?

- <sup>14</sup> and will be instrumented with cold electronics and photon detectors, allowing the interfaces to be  
<sup>15</sup> carefully studied.
- <sup>16</sup> In addition, a small-scale TPC is planned for cold electronics testing at FNAL, and will be in-  
<sup>17</sup> strumented with as many as three 1/2-length PD modules to provide triggering information for  
<sup>18</sup> the TPC and to continue interface studies with the APA and cold electronics. It is envisioned  
<sup>19</sup> that up to three test cycles will be performed prior to the TDR, allowing testing and continued  
<sup>20</sup> development of the ARAPUCA concept.

## <sup>21</sup> 1.2 Photon Detector Efficiency Simulation

- <sup>22</sup> The potential physics performance of PD designs will be evaluated using a full simulation, recon-  
<sup>23</sup> struction, and analysis chain developed for the LArSoft framework. The goal is to evaluate the  
<sup>24</sup> performance in physics deliverables for each of the photon collector designs under consideration.  
<sup>25</sup> The metrics evaluated will include efficiency for determining the time of the event ( $t_0$ ), timing  
<sup>26</sup> resolution, and calorimetric energy resolution for three physics samples: SNB neutrinos, nucleon  
<sup>27</sup> decay events<sup>4</sup>, and beam neutrinos. However, the development of analysis tools to take advan-  
<sup>28</sup> tage of this full simulation chain is fairly recent, so this proposal will only include one test case:  
<sup>29</sup>  $t_0$ -finding efficiency for SNB neutrinos versus the effective area<sup>sssec:photocollectors</sup> 1.1.2.1 of the photon collectors.
- <sup>30</sup> The first step in the simulation specific to the PDS is the simulation of the production of light and  
<sup>31</sup> its transport within the volume to the PDs. Argon is a strong scintillator, producing 24,000  $\gamma$ s/MeV  
<sup>32</sup> at our nominal drift field. Even accounting for the efficiency of the PDs, it is prohibitive to simulate  
<sup>33</sup> every optical photon with GEometry ANd Tracking, version 4 (GEANT4) in every event. So, prior

<sup>4</sup>The most relevant sample is actually the *background* to nucleon decay events. However, efficiently simulating background that can mimic nucleon decays is challenging since they can be quite rare topologies, so it is easier to simulate the nucleon decay signal which should be representative of the background.

1 to the full event simulation, the detector volume is voxelized and many photons are produced in  
 2 each voxel. The fraction of photons from each voxel reaching each photosensor is called the  
 3 *visibility*, and these visibilities are recorded in a 4-dimensional library (akin to the *photon maps*  
 4 used in the DP module simulation. This library includes Rayleigh scattering ( $\lambda = 55\text{ cm}$ [?]),  
 5 absorption ( $\lambda = 20\text{ m}$ ), and the measured collection efficiency versus position of the double-shift  
 6 light-guide bars. When a particle is simulated, at each step it produces charge and light. The light  
 7 produced is distributed onto the various PDs using the photon library as a look-up table and the  
 8 early (6 ns) plus late (1.6  $\mu\text{s}$ ) scintillation time constants are applied. Transport time of the light  
 9 through the LAr is not currently simulated, but is under development.

10 The second step is the simulation of the electronics response. For now, the SiPM signal proce-  
 11 sor (SSP) readout electronics used for PD development and in ProtoDUNE-SP is assumed (see  
 12 Section 1.3.6). Waveforms are produced on each channel by adding an SiPM single-photoelectron  
 13 response shape for each true photon. In addition, other characteristics of the SiPM are included  
 14 such as dark noise, crosstalk and afterpulsing, based on data from device measurements. Dark  
 15 noise, at a rate of 10 Hz for each of the three SiPMs on each channel is include by the addition of  
 16 extra single-photoelectron waveforms. Crosstalk (where a second cell avalanches when a neighbor  
 17 is struck by a photon generated internal to the silicon) is introduced by adding a second photo-  
 18 electron 16.5% of the time when an initial photoelectron is added to the waveform. Additional  
 19 uncorrelated random noise is added to the waveform with an RMS of 2.6 ADC (or approximately  
 20 0.1 photoelectron). The response of the SSP self-triggering algorithm, based on a leading-edge  
 21 discriminator, is then simulated to determine if and when a 7.8  $\mu\text{s}$  waveform will be read out, or  
 22 in the case of the simulation it will be stored and passed on for later processing.

23 The third step is reconstruction, which proceeds in three stages. The first is a “hit finding”  
 24 algorithm that searches for peaks on individual waveforms channel-by-channel, identifying the  
 25 time based on the time of the first peak and the total amount of light collected based on the  
 26 integral until the hit goes back below threshold. The second step is a “flash finding” algorithm  
 27 that searches for coincident hits across multiple channels. All the coincident light is collected into  
 28 a single object that has an associated time (the earliest hit), an amount of light (summed from all  
 29 the hits), and a position on the plane of the anode plane assemblies ( $y$ - $z$ ) that is a weighted-average  
 30 of the positions of the photon collectors with hits in the flash<sup>5</sup>. The final step is to “match” the  
 31 flash to the original event by taking the largest flash within the allowed drift time that is within  
 32 240 cm in the  $y$ - $z$  plane. Since the TPC reconstruction is still in active development, especially for  
 33 low-energy events, we match to the true MC vertex of the event in the analyses presented here.  
 34 This is a reasonable approximation since the position resolution of the TPC will be significantly  
 35 better than that of the PDS.

36 Figure 1.3 (top) shows the efficiency for determining  $t_0$  for events in a typical SNB spectrum  
 37 using the tools above. The changes in effective areas that would correspond to alternative photon  
 38 collection designs are achieved by simply scaling up the total efficiency of the simulated double-  
 39 shift light guide design shown here. The differences in attenuation behaviors within the bars are

<sup>5</sup>Currently, the flash reconstruction does not consider the positions of the hits, only their times. This will need to be updated in the future when we simulate the full-sized far detector,

full detector or SP module?

but for now we are working in a small test geometry that acts as a crude simulation of this kind of constraint.

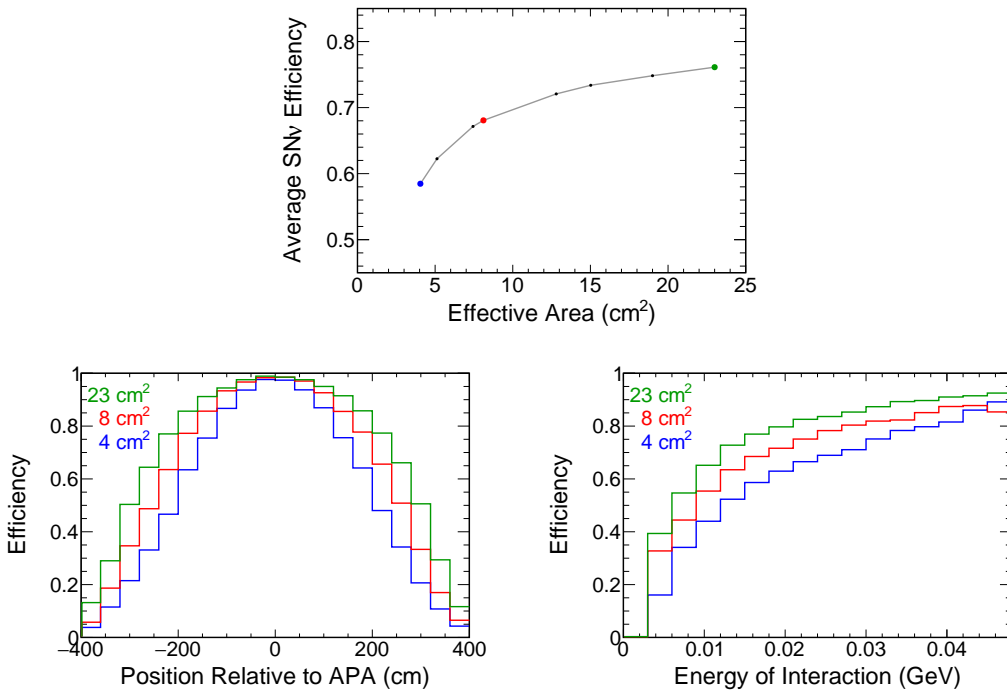


Figure 1.3: Preliminary estimates of the efficiency for finding  $t_0$  for core collapse SNB events vs. the effective area (top), distance from the anode plane (bottom-left), and neutrino energy (bottom-right).

`fig:pds-snefficiency`

1 a second-order effect relative to the total amount of light collected. The efficiency for finding  
 2  $t_0$  for these events increases, but less than linearly as the performance of the light collectors is  
 3 improved. Figures 1.3 (bottom-left) and 1.3 (bottom-right) show how the efficiency varies as a  
 4 function of neutrino energy and distance from the anode plane for three chosen points. Note that  
 5 these algorithms are still in development so there is potential for improvement in the performance  
 6 as development continues.

7 If the correct flash is identified for a SNB event, the resolution on  $t_0$  is excellent, as shown in  
 8 Figure 1.4 – for 95% of the events, the time is identified from the prompt light and the timing  
 9 resolution is better than 100 ns, well within a single TPC time tick. In the remaining 5% of cases  
 10 where a correct flash is matched, the  $t_0$  is biased towards later times (with respect to the true  
 11 event time) by a few  $\mu\text{s}$ , driven by the late light time constant. If the wrong flash is identified the  
 12  $t_0$  found is essentially randomly distributed in the drift time.

13 This preliminary study shows that each of the PD options, with effective area per module currently  
 14 estimated to be in the range 4 to 22  $\text{cm}^2$ , will be able to determine the event  $t_0$  with reasonable  
 15 efficiency and it illustrates the benefit of higher photon detection efficiency.

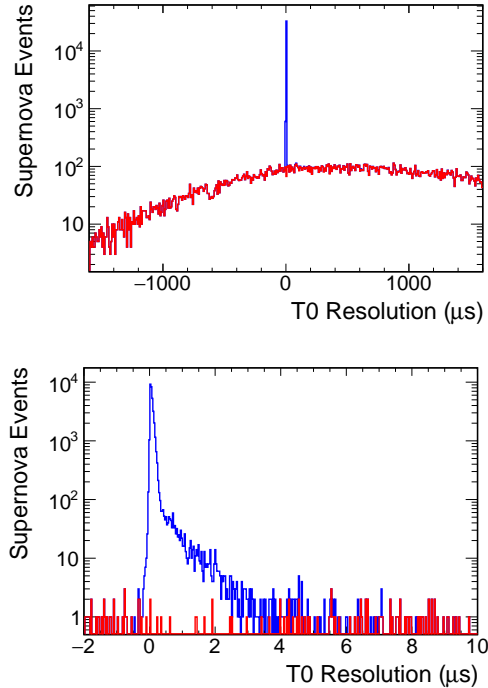


Figure 1.4: Resolution on  $t_0$  for SNB events. These are based on simulation with effective light collector area of  $4\text{ cm}^2$ , which corresponds to the the photon detection efficiency of 0.23% measured for a double-shift light guide module.

fig:pds

## 1.3 Photon Detection System Design

-design

- <sup>1</sup> The principal task of the SP modulePDS is to measure the VUV scintillation light produced by ionizing tracks in the TPC within the geometrical constraints of the APA structure. A commercially available compact solution for photon measurement is the SiPM, however, the response of the devices, which typically peaks in the visible range ( $>400\text{ nm}$ ) is not well-matched to incident 128 nm scintillation photons, so a wavelength shifter or some sort must be employed. In addition, even though production cost and key performance parameters have improved significantly in recent years, the cost of the readout electronics (channel count) and the SiPMs needed to meet the physics requirements of the PDS would be prohibitive.
- <sup>10</sup> The photon collector must optimize the costs of various components of the system while meeting the performance requirements. In practice, this consists of collecting VUV photons over an area of hundreds of square-meters (viewing the entire 10 kt LAr fiducial mass), converting the photons to longer wavelengths and guiding them onto SiPMs that are typically  $O(\text{cm}^2)$ . For reference, an array of 48 SiPMs <sup>6</sup> demonstrated a detection efficiency of 13%, corresponding to an effective area of  $2.2\text{ cm}^2$ .
- <sup>16</sup> A challenge for the PDS is that a full set of requirements is not yet fully defined for one of the

<sup>6</sup>Twelve 4x4 arrays of 3 mm×3 mm sensL C-series coated with 100  $\mu\text{g}/\text{cm}^2$  of tetraphenyl butadiene (TPB), tested in the Fermilab TallBo LAr facility with an alpha source (Am241).

<sup>1</sup> priority physics topics, SNB neutrinos. So the designs strive to demonstrate that at minimum the  
<sup>2</sup> requirements for the accelerator neutrino program, atmospheric neutrinos and nucleon decay will  
<sup>3</sup> be met, while maintaining the flexibility to adjust to the greater demands for the SBN physics.

<sup>4</sup> At the time of the Technical Proposal there are three photon collector options under consideration;  
<sup>5</sup> Figure 1.2 shows how they are incorporated into the TPC anode plane assembly by an identical  
<sup>6</sup> modular mounting scheme. In the following we summarize the design and development status for  
<sup>7</sup> each photon collector option<sup>7</sup>.

### <sup>8</sup> 1.3.1 Photon Collector: ARAPUCA

<sup>9</sup> The ARAPUCA is a device based on a new approach to LAr scintillation photon detection where  
<sup>10</sup> the effective photon detection area is increased by trapping photons inside a box with highly  
<sup>11</sup> reflective internal surfaces until reflections guide them to a much smaller SiPM [?].

<sup>12</sup> Photon trapping is achieved through a novel use of wavelength-shifting and the technology of  
<sup>13</sup> the dichroic shortpass optical filters. These commercially available filters are created by using  
<sup>14</sup> multilayer thin films that in combination have the property of being highly transparent to photons  
<sup>15</sup> with a wavelength below a tunable cut-off while being almost perfectly reflective to photons with  
<sup>16</sup> wavelength above the cut-off. Such a filter coated with either one or two different wavelength-  
<sup>17</sup> shifters, depending on the detailed implementation, forms the entrance window to a flat box with  
<sup>18</sup> internal surfaces covered by highly reflective acrylic foils except for a small fraction of the surface  
<sup>19</sup> that is occupied by active photosensors (SiPMs).

<sup>20</sup> To act as a photon trap, the wavelength-shifter deposited on the outer face of the dichroic filter  
<sup>21</sup> must have its emission wavelength *less* than the cut-off wavelength of the filter, below which  
<sup>22</sup> transmission is typically greater than 95%. These photons pass through the filter where they  
<sup>23</sup> encounter a second wavelength-shifter, either on the inner surface of the filter or coated on the  
<sup>24</sup> reflecting inner surfaces of the box, with an emission spectrum greater than the cut-off wavelength.  
<sup>25</sup> For these photons the reflectivity of the filter is typically greater than 98%, so they will reflect off  
<sup>26</sup> the filter surface (and the inner walls) and so be trapped inside the box with a high probability to  
<sup>27</sup> be incident on an SiPM before being lost to absorption. The concept is illustrated in Figure 1.5,  
<sup>28</sup> in this example the filter cut-off is 400 nm.

<sup>29</sup> The net effect of the ARAPUCA is to amplify the active area of the SiPM used to readout the  
<sup>30</sup> trapped photons. It is easy to show that, for small values of SiPM coverage of the internal surface,  
<sup>31</sup> the amplification factor is equal to  $A = 1/(2(1-R))$ , where R is the average value of the reflectivity  
<sup>32</sup> of the internal surfaces; for an average reflectivity of 0.95 the amplification factor is equal to ten.

<sup>7</sup>For the TDR there will be a baseline design and at most one alternative.

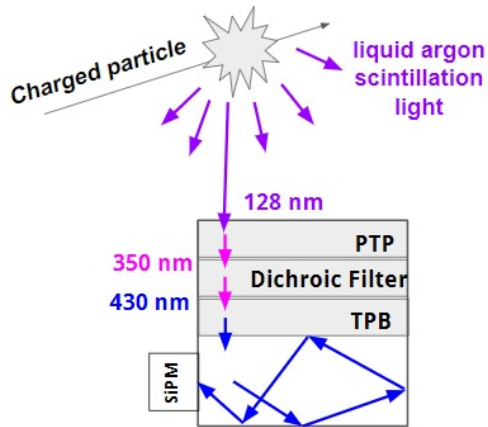


Figure 1.5: Schematic representation of the ARAPUCA operating principle.

fig:arap

### 1.3.1.1 Prototype Measurements

ARAPUCA prototypes with different configurations have been tested in LAr at multiple facilities. In each case, the first wavelength shift of 128 nm scintillation photons down to 350 nm that can pass through the filter substrate was performed by p-TerPhenyl (pTP) evaporated onto the outside of a dichroic filter window.

The first prototype was made of PTFE with internal dimensions of  $3.5\text{ cm} \times 2.5\text{ cm} \times 0.6\text{ cm}$  with a window formed from a dichroic filter with dimensions of  $3.5\text{ cm} \times 2.5\text{ cm}$  and wavelength cut-off at 400 nm. TetraPhenyl-Butadiene (TPB) was evaporated onto the internal side of the filter where it absorbs the shifted 350 nm photons and reemits around 430 nm. Trapped light is detected by a single  $0.6\text{ cm} \times 0.6\text{ cm}$  sensL SiPM mod C60035<sup>8</sup>. The device was installed inside a vacuum tight stainless-steel cylinder closed by two CF100 flanges. The cylinder was deployed inside a LAr open bath, vacuum pumped down to a pressure around  $10^{-6}\text{ mbar}$  and then filled with one liter of ultra-pure LAr<sup>9</sup>.

Scintillation light emission was produced by an alpha source<sup>10</sup> installed in front of the ARAPUCA immersed in LAr. Signals were read out through an Aquiris<sup>11</sup> PCI board and stored on a computer. Figure 1.6 shows photographs of the ARAPUCA and cryogenic system at the Brazilian Synchrotron Light Laboratory (LNLS).

The detection efficiency of the ARAPUCA was calculated by determining the number of photoelectrons detected corresponding to the end point of the  $\alpha$  spectrum and comparing it with the expected number of photons impinging on the acceptance window for that particular energy value ( $\sim 4.3\text{ MeV}$ ). This depends only on known properties of LAr and on the solid angle subtended by

<sup>8</sup><http://sensl.com/products/c-series/>

<sup>9</sup>Argon 6.0, less than 1 ppm total residual contamination.

<sup>10</sup>A  $^{238}\text{U}$ -Al alloy in the form of a metallic foil, with alpha particle emission of 4.267 MeV.

<sup>11</sup>Aquiris High-Speed Digitizer products; <http://www.acqiris.com/>.



Figure 1.6: ARAPUCA test at the Brazilian Synchrotron Light Laboratory

LNLS\_tes

<sup>1</sup> the ARAPUCA window. A detection efficiency at the level of 1.8% was measured, consistent with  
<sup>2</sup> MC expectations for the this configuration[?].

<sup>3</sup> The next several prototypes were tested under cryogenic conditions at Fermilab. The first, per-  
<sup>4</sup> formed in mid-2016 at the Proton Assembly Building (PAB) at the ScENE cryogenic test facility,  
<sup>5</sup> had dimensions of  $5.0\text{ cm} \times 5.0\text{ cm} \times 1.0\text{ cm}$  with a dichroic window of  $5.0\text{ cm} \times 5.0\text{ cm}$  with a cut-off  
<sup>6</sup> of 400 nm which was deposited with pTP and TPB. However, in this case, two of sensL SiPMs mod  
<sup>7</sup> C60035 were installed inside the box. The ARAPUCA was again deployed inside a vacuum-tight  
<sup>8</sup> cryostat filled with ultrapure LAr. An  $^{241}\text{Am}$  alpha source was positioned in front of the window  
<sup>9</sup> of the device 5 cm from its center. The efficiency of the ARAPUCA was estimated taking into  
<sup>10</sup> account that the alpha particles from this source have a monochromatic energy of about 5.4 MeV.  
<sup>11</sup> The estimated efficiency in this case was approximately 1%, a factor two below the expected value;  
<sup>12</sup> this is attributed to the sub-optimal quality and uniformity of the pTP and TPB films, and to the  
<sup>13</sup> lack of reflectivity of the inner PTFE surfaces in this early prototype.

<sup>14</sup> The next set of tests was performed at the beginning of 2017 at the PAB, but using the TallBo  
<sup>15</sup> facility, which is large enough to allow testing of several devices at a time. Eight different ARA-  
<sup>16</sup> PUCA cells with filters from different manufacturers, different reflectors, and different dimensions  
<sup>17</sup> were tested. Scintillation light was again produced by alpha particles emitted by an  $^{241}\text{Am}$  source  
<sup>18</sup> mounted on a holder that could be moved with an external manipulator in order to place it in  
<sup>19</sup> front of each prototype. The detection efficiencies of these ARAPUCAs ranged from 0.4% to 1.0%.

<sup>20</sup> The most recent measurements were performed in the TallBo facility at the end of 2017 with an  
<sup>21</sup> array of eight ARAPUCAs together with two reference bars (double-shift light guide design). The  
<sup>22</sup> data analysis for the ARAPUCA array is currently underway.

### <sup>23</sup> 1.3.1.2 ARAPUCA in ProtoDUNE-SP

<sup>24</sup> Two arrays of ARAPUCA modules will be operated inside ProtoDUNE-SP to test the devices in  
<sup>25</sup> a large-scale experimental environment and allow direct comparison of their performance with the

- <sup>1</sup> light guide designs.
- <sup>2</sup> Each ProtoDUNE-SP ARAPUCA module array is composed of sixteen cells where each cell is an  
<sup>3</sup> ARAPUCA box with dimensions of  $8\text{ cm} \times 10\text{ cm}$ ; half of the cells have twelve SiPMs installed on the  
<sup>4</sup> bottom side of the cell and half have six SiPMs. The SiPMs have active dimensions  $0.6\text{ cm} \times 0.6\text{ cm}$   
<sup>5</sup> and account for 5.6% (12 SiPMs) or 2.8% (6 SiPMs) of the area of the window ( $7.8\text{ cm} \times 9.8\text{ cm}$ ).  
<sup>6</sup> The SiPMs are passively ganged together, so that only one readout channel is needed for each  
<sup>7</sup> ARAPUCA grouping of 12 SiPMs (the boxes with six SiPMs are ganged together to form 12-  
<sup>8</sup> SiPM units) so a total of 12 channels is required per array. Studies are underway to investigate  
<sup>9</sup> active ganging that would permit combining signals from multiples boxes as required to reduce the  
<sup>10</sup> number of electronics channels and cables (currently in the SP module 10 kt, we anticipate being  
<sup>11</sup> restricted to four readout channels per PD module). The total width of a module is 9.6 cm, while  
<sup>12</sup> the active width of an ARAPUCA is 7.8 cm, the length is the same as the light guide modules  
<sup>13</sup> ( $\sim 210\text{ cm}$ ). The first ARAPUCA array installed in ProtoDUNE-SP is shown in Figure 1.8. If the  
<sup>14</sup> ARAPUCA cells achieved the same detection efficiency as earlier prototypes (1.8%), the effective  
<sup>15</sup> area of an ARAPUCA module will be approximately  $23\text{ cm}^2$ .



Figure 1.7: Full-scale ARAPUCA for ProtoDUNE-SP during assembly. SiPMs are visible in the sixteen cells before the installation of reflecting foils, coated filter windows, and readout cabling.

fig:arpca\_array

### <sup>16</sup> 1.3.1.3 X-ARAPUCA

- <sup>17</sup> X-ARAPUCA represents an alternative line of development with the aim of further improving the  
<sup>18</sup> collection efficiency, while retaining the same working principle, mechanical form factor and active  
<sup>19</sup> photo-sensitive coverage. X-ARAPUCA is effectively a hybrid solution between the ARAPUCA  
<sup>20</sup> and the wavelength-shifting light guide concepts, where photons trapped in the ARAPUCA box  
<sup>21</sup> are shifted and transported to the readout via total internal reflection in a short light guide placed

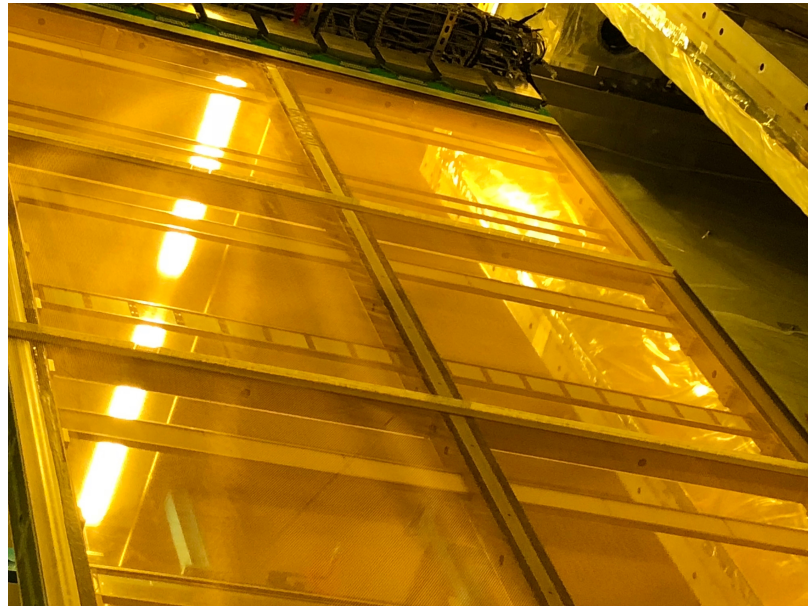


Figure 1.8: ARAPUCA array in ProtoDUNE-SP.

fig:arap

1 inside the box. This solution minimizes the number of reflections on the internal surfaces of the  
 2 box and thus the probability of photon loss. Simulations suggest that this modification will lead  
 3 to a rather significant increase of the collection efficiency, to around 60%, so the photon detection  
 4 efficiency including the SiPM response could approach 20%.

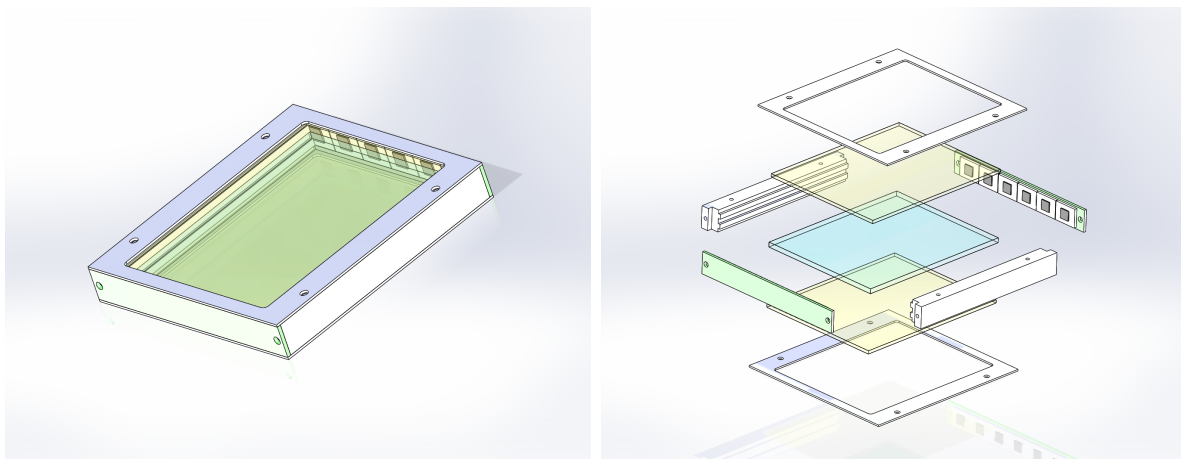


Figure 1.9: X-ARAPUCA design: assembled cell (left), exploded view (right). The size and aspect ratio of the cells can be adjusted to match the spatial granularity required for a PD module.

fig:pds-

5 In the X-ARAPUCA design, Figure 1.9, the inner shifter coating/lining over the reflective walls  
 6 of the box is replaced by a thin wavelength-shifting light guide slab inside the box, of the same  
 7 dimensions of the acceptance filter window and parallel to it. The SiPM arrays are installed  
 8 vertically on the sides of the box, parallel to the light guide thin ends. In this way a fraction of the  
 9 photons will be converted inside the slab and guided to the readout, other photons, e.g., those at  
 10 small angle of incidence below the critical angle of the light guide slab, after conversion at the slab  
 11 surface will remain trapped in the box and eventually collected as for the standard ARAPUCA.

fig:pds-x-arapuca-cell

- 1 A full-sized X-ARAPUCA prototype is under development. The light guide is a 3 mm thick TPB-  
 2 doped acrylic plate. Two readout boards, each with several passively ganged SiPMs in a strip  
 3 configuration, are mounted along the thin edges of the box and their ganged signals are combined  
 4 into a single channel readout. The aspect ratio of the cells can be adjusted to match the required  
 5 spatial granularity for the PD module.

### 6 1.3.1.4 ARAPUCA Configuration in DUNE 10 kt

7 The modular arrangement of the SP module TPC calls for a configuration across the width of the  
 8 cryostat starting with an APA plane against one cryostat wall, and following with anode plane  
 9 assemblies and CPAs arranged as follows: APA-CPA-APA-CPA-APA. This means that the central  
 10 APA will collect charge and see scintillation light from LAr volumes on both sides, whereas those  
 11 by the wall collect from only one side. While the ARAPUCA modules deployed in ProtoDUNE-  
 12 SP collect light from only one direction, several ARAPUCA configurations under development are  
 13 capable of collecting light from both sides (including the X-ARAPUCA concept). The optimal  
 14 configuration of ARAPUCA modules has not yet been determined, but the basic design allows for  
 15 both single-sided and double-sided cells with no impact on the APA design.

### 16 1.3.2 Photon Collector: Dip-Coated Light Guides

17 The *dip-coated* light guide design is mechanically the simplest of the three options. Figure 1.10  
 18 illustrates the process by which LAr scintillation photons are converted and detected in this approach.  
 19 VUV scintillation photons incident on the bar are absorbed and wavelength-shifted to blue (~430 nm) by the TPB-based coating on the surface of the bar. A portion of this light is  
 20 captured in the bar and guided to one end through total internal reflection where it is detected  
 21 by an array of SiPMs, whose PDE is well-matched to the blue light. Dimensions of the bars in  
 22 ProtoDUNE-SP are: 209.3 cm × 8.47 cm × 0.60 cm. Since the bar is coated on all sides, in the SP  
 23 module it can be employed both in the wall anode plane assemblies as well as in the center APA  
 24 array where scintillation light approaches from two drift volumes.

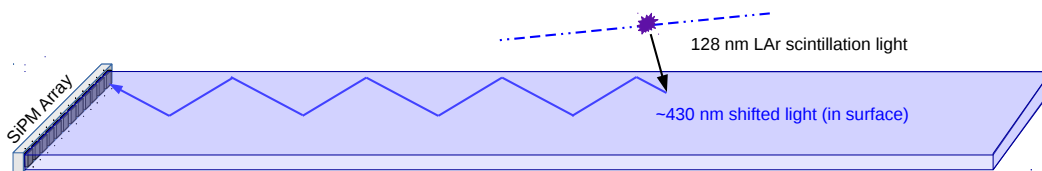


Figure 1.10: Schematic of scintillation light detection with dip-coated light guide bars.

26 The dipping process and coating formula have undergone a series of development iterations [?],  
 27 with the bars undergoing extensive testing at both room and cryogenic temperatures. As a part  
 28 of the production process, the attenuation of each dip-coated light guide bar is measured at room  
 29 temperature in a dark box with a UV LED; 80% of the bars measured have an attenuation length  
 30 in air of 6 m or greater. Attenuation measurements on full-length bars have not yet been performed

Moss:2014ota

- <sup>Moss:2014ota</sup>  
<sup>Moss:2016yhb</sup>
- 1 in LAr, but a model presented in [?] predicts effective attenuation lengths greater than 2 m [?].
  - 2 The general features of this model were validated by measurements using  $^{210}\text{Po}$  alpha sources in
  - 3 the TallBo cryogenic test stand at FNAL.
  
  - 4 A further validation of the bar performance came from a set of measurements taken in the TallBo
  - 5 cryostat containing the four initial candidate photon collector technologies using alpha sources and
  - 6 tracked cosmic ray muons, allowing side-by-side comparisons [?]. As a result, the two approaches
  - 7 that showed the highest promise, dip-coated and double-shift light guides (described in the next
  - 8 section), were continued for further development since these had similar photon detection efficiency,
  - 9  $\sim 0.1\%$ , that was significantly higher than the other two.
  
  - 10 A simple improvement to the bar performance is to read out both ends of the bar rather than a
  - 11 single end as is the case for bars deployed in ProtoDUNE-SP. In addition, test bars have been
  - 12 produced with a higher TPB-to-acrylic ratio, which may have a higher conversion efficiency without
  - 13 introducing a reduction in attenuation length. These improvements could increase the photon
  - 14 detection efficiency of the dip-coated light guide by more than a factor of two.

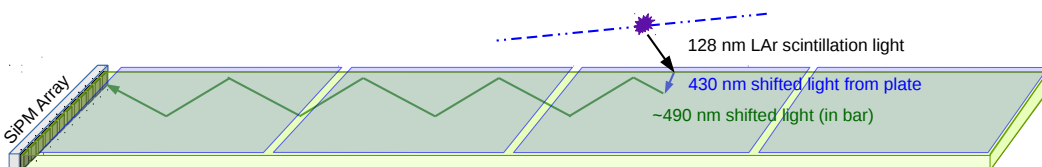
### <sup>15</sup> 1.3.3 Photon Collector: Double-Shift Light Guides

<sup>-pc-bar2</sup>

- 16 In the early implementations of the dip-coated light guide development there was a strong de-
- 17 pendence of the light yield along the length of the bar, presumed to be due to the impact of the
- 18 coating on the total internal reflection efficiency. In an effort to mitigate this effect, the *double-shift*
- 19 light guide design decouples the process of converting VUV photons to optical wavelengths from
- 20 the transportation of photons along the bars. This is achieved by positioning an array of acrylic
- 21 plates coated with TPB in front of a high-quality commercial polystyrene light guide doped with
- 22 a second wavelength-shifting compound.

<sup>fig:pds-doubleshiftlg-cartoon</sup>  
<sup>23</sup> Figure 1.11 illustrates the double-shift light guide concept. VUV scintillation photons incident on

- 24 the acrylic plates are converted to blue wavelengths ( $\sim 430 \text{ nm}$ ) and a fraction of these blue photons
- 25 penetrate the light guide and are converted to green ( $\sim 490 \text{ nm}$ ). The re-emission of these green
- 26 photons, taken to be a Lambertian distribution (isotropic luminance), leads to some becoming
- 27 trapped by total internal reflection within the light guide and transported to the end of the light
- 28 guide where they are detected by an array of SiPMs.



<sup>fig:pds-</sup> Figure 1.11: Schematic of the principle of a double-shift light guide.

<sup>29</sup> The radiator plates are formed by spray-coating TPB on the outer surface of acrylic plates, as

<sup>ssec:tdsp-pd\_pc-prod-par2</sup>

- 30 described in Section 1.4.1.3. A full-scale double-shift light collector module consists of six radi-
- 31 ator plates mounted on each face of the wavelength-shifting light guide (12 plates total). The

<sup>1</sup> 210 cm × 8.6 cm light guide is fabricated by Eljen Technologies<sup>12</sup> and consists of a polystyrene bar  
<sup>2</sup> doped with the EJ-280 wavelength shifter. EJ-280 features an absorption spectrum that is well  
<sup>3</sup> matched to the TPB emission spectrum so wavelength-shifted photons emitted from the plates are  
<sup>4</sup> absorbed with good efficiency.

<sup>5</sup> For most of the testing and the ProtoDUNE-SP modules, the SiPM array used 0.6 cm × 0.6 cm  
<sup>6</sup> sensL C-series MicroFC-60035-SMT SiPMs. These were originally selected since they were a good  
<sup>7</sup> match for the TPB emission spectrum on the dip-coated bars. However, they have a photon  
<sup>8</sup> detection efficiency between 20%–35% across the emission spectrum of the EJ-280 wavelength  
<sup>9</sup> shifter, compared to up to 40% at the peak, so selecting a different device with a better-matched  
<sup>10</sup> photon detection efficiency would improve the performance of the double-shift design.

<sup>11</sup> The double-shift light guide design has undergone a series of development iterations to improve  
<sup>12</sup> its performance, carried out at Indiana University (IU) and at Fermilab’s cryogenic and vacuum  
<sup>13</sup> test facility in the PAB. Comparative testing of light guide designs at PAB in mid-2015 demon-  
<sup>14</sup> strated the viability of the double-shift light guide concept [?]. An improved design similar to  
<sup>15</sup> that deployed at ProtoDUNE-SP was studied at the Blanche test stand at Fermilab in September  
<sup>16</sup> of 2016 with a complementary component-wise analysis program at IU afterward, as detailed in  
<sup>17</sup> [?]. The attenuation characteristics of this light guide were measured at IU, while the detection  
<sup>18</sup> efficiency for incident LAr scintillation photons was measured with a vacuum-ultraviolet (VUV)  
<sup>19</sup> monochromator at IU and using scintillation light from cosmic rays at the Blanche test stand.

<sup>20</sup> Analysis of the double-shift light guide’s attenuation properties determined an attenuation pro-  
<sup>21</sup> file in LAr characterized by a double-exponential function of the form  $f(z) = A \exp(-z/\lambda_A) +$   
<sup>22</sup>  $B \exp(-z/\lambda_B)$  with  $z$  the distance from the instrumented end and parameters  $A = 0.29$ ,  $\lambda_A = 4.3$  cm,  
<sup>23</sup>  $B = 0.71$ , and  $\lambda_B = 225$  cm [?]. The effective attenuation length of ~2 m is comparable to the width  
<sup>24</sup> of an APA when the double-shift light guide is deployed in LAr.

Using both direct measurement with the monochromator and scintillation light, the photon detection efficiency of this detector was determined to be 0.48% at the end close to the SiPM readout. The total effective area for detecting VUV scintillation photons in this module can be determined by integrating the product of this efficiency and the attenuation function over the area of the detector:

$$A_{eff} = (0.0048)(8.5\text{cm}) \int_{0\text{cm}}^{210\text{cm}} dz (0.29 \exp(-z/4.3\text{cm}) + 0.71 \exp(-z/225\text{cm}))$$

<sup>25</sup> This corresponds to an effective area for detecting VUV scintillation photons of  $4.1 \text{ cm}^2$  per mod-  
<sup>26</sup> ule per drift volume, which corresponds to overall 0.23% photon detection efficiency for events  
<sup>27</sup> occurring on one side of the APA. Since the radiator plates are deployed on both faces of the  
<sup>28</sup> light guide, modules in the center APA array are sensitive to scintillation light from the two drift  
<sup>29</sup> volumes on either side.

<sup>30</sup> There are several ways that the current design could be improved. The double-shift light guide  
<sup>31</sup> deployed in the ProtoDUNE-SP anode plane assemblies is constrained to read out at a single end.  
<sup>32</sup> Proposed changes to the APA size and cabling routing scheme for the SP module would allow for  
<sup>33</sup> a second array of SiPMs at the opposite end of the light guide, which would almost double the

<sup>12</sup><http://www.eljentechnology.com>

1 performance of the photon detection system. A SiPM with a wavelength-dependent PDE that is  
 2 better matched to the EJ-280 emission spectrum would also improve the efficiency. Simulations of  
 3 the transport of light within the light guide suggest that applying a highly reflective coating to the  
 4 long, narrow inactive sides of the light guide would improve the attenuation function and increase  
 5 the effective area of the light guide module. These effects combined lead to a potential increase of  
 6 the effective area up to four times the current prototypes, approaching 1% detection efficiency.

### **7 1.3.4 Additional Techniques to Enhance Light Yield**

**8** Though we anticipate that the designs described in the previous sections will meet the PD perfor-  
**9** mance requirements we do not yet have final designs and so we have also considered options for  
**10** enhancing the light yield if that becomes necessary. Some of the initial ideas, such as deploying a  
**11** large array of Winston-cone style reflectors focusing light onto SiPMs throughout the entire area  
**12** enclosed by the APA frame, would require a significant change in the APA production and assem-  
**13** bly planning and so will become increasing untenable. However, one option being investigated in  
**14** parallel with the photon collector modules design is to convert the scintillation light falling on the  
**15** cathode plane into the visible wavelengths, which in turn illuminates photon detectors embedded  
**16** in the APA, as is currently envisioned.

**17** A motivation for this approach is that, due to geometric effects, the baseline PDS design will  
**18** result in some non-uniformity of light collection along the drift direction. Light emitted from  
**19** interactions close to the anode plane assemblies has an order of magnitude larger chance of being  
**20** detected compared to interactions close to the CPA. This effect can be mitigated by installing  
**21** wavelength-shifter (TPB) coated dielectric reflector foils on the cathode planes. Light impinging  
**22** on these foils is wavelength-shifted into visible wavelengths and reflected from the underlying foils.  
**23** This light can subsequently be detected by photon detectors placed in the anode plane assemblies  
**24** provided they are sensitive to visible light (which is not the case for the current photon collector  
**25** modules). Fig. 1.12, shows that if the APA photon collectors are capable of recording both direct  
**26** scintillation light and the visible light from the CPA, there is an enhancement of the total light  
**27** collection close to the cathode (black points), which will increase the detection efficiency in that  
**28** region. Another benefit is the increase in uniformity - this can enable calorimetric reconstruction  
**29** with scintillation light, which would enhance the charge-based energy reconstruction as well as  
**30** increase the efficiency of triggering on low energy signals. Introducing the foils on the cathode  
**31** may also enable drift position resolution using only scintillation light. This requires the photon  
**32** detectors to be able to differentiate direct VUV light from re-emitted visible light (e.g. two different  
**33** PD detector types) and good enough timing of arrival of first light.

**34** Coated reflector foils are manufactured through low-temperature evaporation of TPB on dielectric  
**35** reflectors e.g. 3M DM2000 or Vikuiti™ ESR. Foils prepared in this manner have been successfully  
**36** used in dark matter detectors such as WArP<sup>[?]</sup>. Recently they have been shown to work in  
**37** LArTPCs at neutrino energies, namely in the LArIAT test-beam detector<sup>[?]</sup>. In LArIAT they  
**38** have been installed on the field-cage walls and, during the last run, on the cathode.

**39** The necessity to record both VUV and visible photons in the Photon Collectors would require  
**40** a change in the current design but is conceptually possible. For example, if the cathode plane

were coated with tTP, some of the ARAPUCA modules could be constructed without the pTP coating on the outer surface of the filter and benefit from the same photon trapping effect but these cells would no longer be sensitive to direct scintillator light. Understanding the impact of these competing effects on the physics is under study by the simulation group and the feasibility of coating the cathode with a dielectric medium is being investigated with the DUNE HV consortium.

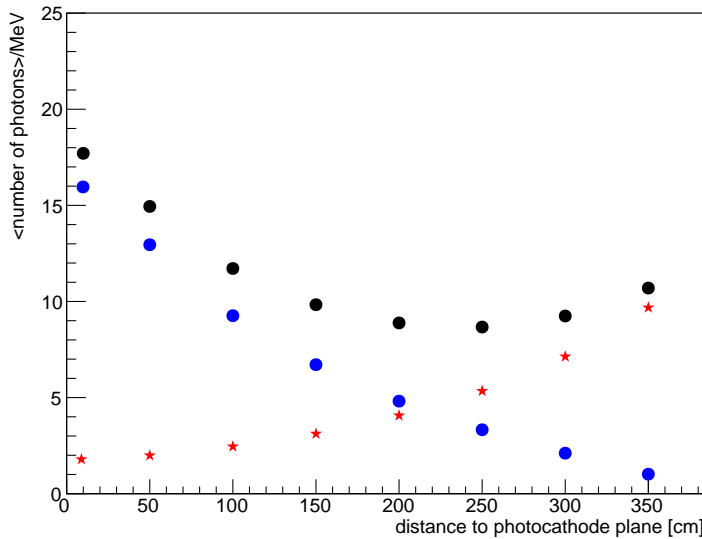


Figure 1.12: Predicted light yield in with WLS-coated reflector foils on the CPA. Blue points represent direct VUV light impinging on the PDs assuming a 0.42% photon detection efficiency and 70% wire mesh transmission; red stars - represent scintillation light that has been wavelength-shifted and reflected on the CPA assuming the same photon detection efficiency. Black points show the sum of these two contributions (which would require twice the number of PD modules in the current APA configuration).

fig:ly\_w

### 1.3.5 Silicon Photosensors

The SP module PDS uses a multi-step approach to scintillation light detection with final stage of conversion into electrical charge performed by silicon photomultipliers (SiPM). Robust photon detection efficiency, low operating voltages, small size and ruggedness make their use attractive in the SP design where the photon detectors must be accommodated inside the APA frames. As implemented in ProtoDUNE-SP, there are twelve  $6 \times 6 \text{ mm}^2$  SiPMs per bar and 6-12 per ARAPUCA box. With this configuration, a 10 kt SP module with 150 anode plane assemblies, each with 10 PD modules, would contain 18,000-36,000 (single or double-ended readout) SiPMs for the light guide designs and 10-20 times more for the higher granularity ARAPUCA design. This corresponds to approximately  $1\text{-}13 \text{ m}^2$  of active SiPM surface area.

In the following we summarize the most salient guiding principles and requirements for this SiPM-based photodetection system.

- The full suite of SiPM requirements (number of devices, spectral sensitivity, dynamic range, triggering, zero-suppression threshold etc.) is determined by the physics goals and the ph-

ton collection implementation. As discussed in Section 1.1.1, the requirements for SNB neutrinos are not yet fully established however, R&D carried out to date indicates that devices from several vendors have the performance characteristics close to that needed for the PDS (see Table 1.3). Nearly one thousand of several types of these devices are used in the ProtoDUNE-SP PD<sup>13</sup>, which will provide an excellent test bed for evaluating and monitoring SiPM performance in a realistic environment over a period of months.

- A key requirement is to ensure the mechanical and electrical integrity of these devices in a cryogenic environment. However, currently, catalogue devices for most vendors are certified for operation only down to -40°C. It is essential to be in close communication with vendors in the design, fabrication and SiPM packaging certification stages to ensure that the device will be robust and reliable for long-term operation in a cryogenic environment. Two sources have expressed interest to engage with the consortium in this fashion with the goal of having the vendor warranty the product for our application: Hamamatsu Photonics K.K., a large well-known commercial vendor in Japan and Fondazione Bruno Kessler (FBK) in Italy, an experienced developer of solid state photosensors that typically licenses its technology and which is partnering with the DarkSide collaboration to develop a devices with very similar requirements as DUNE. Contact with other vendors and experiments using this technology in a similar environment is being pursued.
- Comparative performance evaluation of promising SiPM candidates from multiple vendors will need to be carried out in parallel over the next year. This evaluation will need to address inherent device characteristics (gain, dark rate, x-talk, after-pulsing etc), which are common to all three photon collector options, along with ganging performance, form factor, spectral response, and mechanical mounting options that may have different optimization for the two light guide design and ARAPUCA. Experience acquired from ProtoDUNE-SP construction and operation will inform QA/QC plans for the full detector, which will need to be delineated in detail.
- The optimal SiPM may depend on the photon collector option selected. All options currently being considered involve shifting the 128 nm LAr scintillation light to longer wavelengths, but each may present a different spectral distribution to the SiPM. In this case, final selection of the SiPM might be delayed to allow an optimal match to the photon collector. However, we would not expect this fine-tuning to be more than a 15-20% effect, so it is not a driving factor.
- For the light guide photon collector designs, the SiPM packaging should allow for tileable arrays to be constructed to facilitate high packing efficiency across the end of the bars and efficient space utilization inside the APA frame.
- Current candidate SiPMs have an area of less than 1 cm<sup>2</sup>, a much finer granularity than needed. In addition, the cold feedthrough size and space in the anode plane assemblies for cable runs limits the number of PD signal and power cables. These constraints, and other considerations, imply that the signal output of SiPMs must be electrically ganged.

<sup>13</sup>ProtoDUNE-SP PDS uses 516 sensL MicroFC-60035C-SMT, 288 Hamamatsu MPPC 13360-6050CQ-SMD with cryogenic packaging, 180 Hamamatsu MPPC 13360-6050VE.

The degree of ganging depends on the photon collectors technology and currently ranges from 6 SiPMs for the light guides to 48 or more for the ARAPUCA modules. Whether simple passive-ganging (wiring the outputs together) will suffice or if active-ganging (with active components) is under investigation as a joint responsibility of the photon sensor and electronics working groups (see Section 1.3.6.1 for more details).

- The terminal capacitance of the sensors strongly affects the signal-to-noise when devices are ganged in parallel and so is a factor in SiPM selection, and may ultimately determine the maximum number of individual sensors that can be ganged this way.

Table 1.3: Candidate Photosensors Characteristics.

	Hamamatsu	sensL	KETEK	Advansid
Series part #	S13360	DS-MicroC	PM33	NUV-SiPMs
Vbr range	48 V to 58 V	24.2 V to 24.7 V	27.5 V	24 V to 28 V
Vop range	Vbr + 3 V	Vbr +1 V to +3 V	Vbr+2V to +5 V	Vbr +2 V to +6 V
Temp. dependence	54 mV/K	21.5 mV/K	22 mV/K	26 mV/K
Gain	$1.7 \times 10^6$	$3 \times 10^6$	$1.74 \times 10^6$	$3.6 \times 10^6$
Pixel size	50 $\mu\text{m}$	10 $\mu\text{m}$ to 50 $\mu\text{m}$	15 $\mu\text{m}$ to 25 $\mu\text{m}$	40 $\mu\text{m}$
Sizes	2x2 mm 3x3 mm 6x6 mm	1x1 3x3 6x6	3x3	4x4 3x3
Wavelength	320 to 900 nm	300 to 950 nm	300 to 950 nm	350 to 900 nm
PDE peak wavelength	450 nm	420 nm	430 nm	420 nm
PDE @ peak	40%	24% to 41%	41% at Vov=5 V	43%
DCR @0.5PE	2 to 6 MHz	0.3 kHz to 1.2 MHz	100 kHz at Vovr=5 V	100 kHz/mm <sup>2</sup>
Crosstalk	< 3%	7%	15%	< 4% (correlated noise)
Afterpulsing		0.20%	<1%	<4%
Terminal capacitance	1300 pF	3400 pF	750 pF	800 pF
Lab experience	Good experiences from Mu2e and ARAPUCA	Crack at temps. after specifications change		

## 1 1.3.6 Electronics

### 2 1.3.6.1 Introduction

3 The PD design requires the readout system to collect and process electrical signals from photosen-  
4 sors reading out the light collector bars, to provide interface with trigger and timing systems to  
5 support data reduction and classification, and to enable data transfer to offline storage for physics  
6 analysis.

7 The readout system must enable the measurement of the  $t_0$  of non-beam events with deposited en-  
8 ergy above 10 MeV. This capability will also enhance beam physics, by recording interaction time  
9 of events within beam spill to help separate against potential cosmic background interactions. Two  
10 main methods of data collection are currently considered: self-triggered integrated charge readout  
11 and wave form digitization. Charge integration appears to be a likely candidate at this point in  
12 our development, as it offers the potential for a simpler, commercially available charge integra-  
13 tion circuit and perhaps a smaller, less-expensive cable plant to read it out. Physics simulation  
14 studies are currently underway to determine if pulse-shape discrimination will be required, which  
15 would provide the capability to record both prompt and delayed components of scintillation light  
16 (characteristic times of 6 ns and 1.3  $\mu$ s), the latter consisting mostly of single photoelectrons and  
17 thus place stringent requirements on signal-to-noise performance. The photon detector collects a  
18 limited amount of light, so it could be beneficial to collect the light from both excited states. Since  
19 this requirement has not yet been established the option is kept open in the electronics design.

20 All photon collector options will require some level of electrical ganging of the SiPMs, either passive  
21 direct connection of the SiPM outputs or active (cold signal summing and possibly amplification).  
22 To that end we desire a system where the ganging is maximized to minimize the electronics  
23 channel count while maintaining adequate redundancy and granularity, as well as readout system  
24 performance. This represents a significant interface between the electronics, photosensor and light  
25 collector designs, and will be a main focus of our development and optimization work up to the  
26 TDR.

27 Technical factors that affect performance of the ganging system are the characteristic capacitance of  
28 the SiPM and the number of SiPMs connected together, which together dictate the signal to noise  
29 ratio and affect the system performance and design considerations. Selection of the ganging option  
30 will include passive or active solutions, where the active circuitry may require cold components  
31 such as an amplifier in the LAr volume. Design options with active cold components will need  
32 to address issues of power dissipation and potential risks of single-point failures of multi-channel  
33 devices inside the cryostat. In the case of passive ganging, analog signals are transmitted outside  
34 of the cryostat for processing and digitalization. Successful demonstrations of passive ganging  
35 at LAr temperatures have been made for groups of four and twelve 6x6 mm Micro-FC-60035C-  
36 SMT C series, and groups of 2, 4, 8, and 12 Hamamatsu MPPCs (S13360-6050PE) at 25°C, -  
37 70°C and 77K. Active ganging has been demonstrated for an array of 12 sensL 4×4 arrays of  
38 3 mm×3 mm sensL C-series SiPMs (48 in all) and 72 SiPMs mounted in a hybrid combination of  
39 passive and active ganging using 6 mm×6 mm MPPCs with a low noise operational amplifier—this  
40 design combines 12 active branches into the op-amp, where each branch has 6 MPPCs in a parallel

- <sup>1</sup> passive-ganging configuration.
- <sup>2</sup> Typically, arrival time and total charge are the key parameters to be obtained from a detector.
- <sup>3</sup> Extraction of these parameters is possible using analog or digital systems. Charge preamplifiers
- <sup>4</sup> will be connected to the output of the detector to integrate current producing a charge proportional
- <sup>5</sup> output. In the case of digital systems an amplifier is needed to adjust the detector output signal
- <sup>6</sup> level to the input of an Analog to Digital Converter. In both systems, performance parameters
- <sup>7</sup> related to sampling rate, number of bits, power requirements, signal to noise ratio, and interface
- <sup>8</sup> requirements should be evaluated to arrive to selected solution. Pulse shapes can be fully analyzed
- <sup>9</sup> to improve detection of a new physics but it will have an important impact on the digitalization
- <sup>10</sup> frequency.

### <sup>11</sup> 1.3.6.2 ProtoDUNE-SP Electronics

<sup>12</sup> A dedicated photon-detector readout system, presented schematically in Figure 1.13(left), was  
<sup>13</sup> developed for ProtoDUNE-SP, which will be operational in the second half of 2018. Twenty-four  
<sup>14</sup> custom SiPM Signal Processor (SSP) units were produced to read out the 58 light guide and 2  
<sup>15</sup> ARAPUCAs photon collectors. An SSP contains of twelve readout channels packaged in a self-  
<sup>16</sup> contained 1U module; four SSPs are shown in Figure 1.13(right). <sup>fig:fig-pds-readout</sup>

<sup>17</sup> A passive ganging scheme with three SiPMs ganged together was chosen for the light guides (4 SSP  
<sup>18</sup> channels for each bar) and groups of twelve SiPMs are passively ganged for the two ARAPUCA  
<sup>19</sup> modules (12 SSP channels per module). The unamplified analog signals from the SiPMs are  
<sup>20</sup> transmitted to outside the cryostat for processing and digitization over an approximately 25 m  
<sup>21</sup> cable to the SSP outside the cryostat. Each channel receives the SiPM signal into a termination  
<sup>22</sup> resistor that matches the characteristic impedance of the signal cable followed by a fully-differential  
<sup>23</sup> voltage amplifier and a 14-bit, 150-MSPS analog-to-digital converter (ADC) that digitizes the SiPM  
<sup>24</sup> signal waveforms.

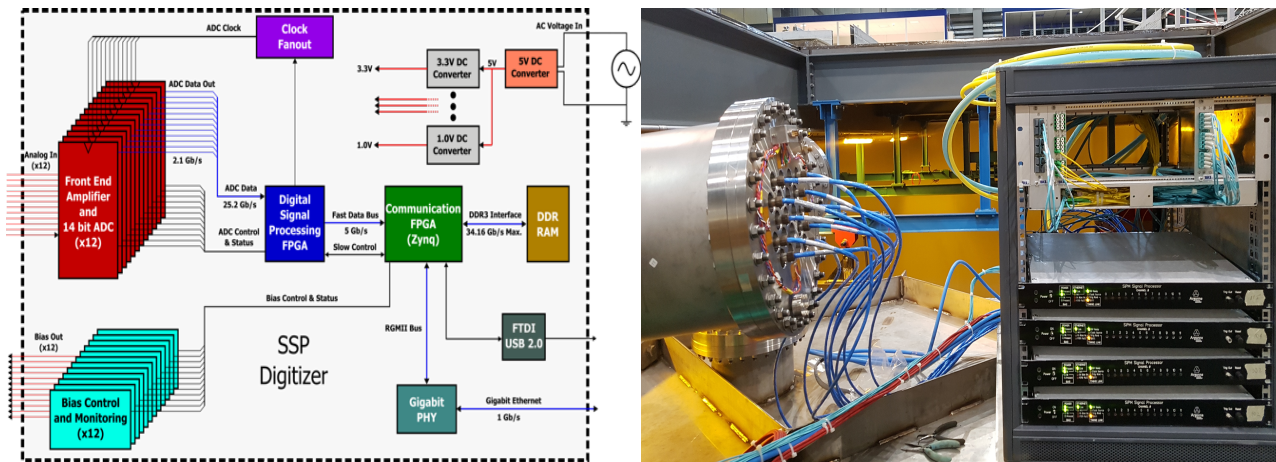


Figure 1.13: Block diagram of the ProtoDUNE-SP photon detector readout module (left). Photon detector readout system operational at ProtoDUNE-SP (right).

- <sup>25</sup> In the standard mode of operation, the module performs waveform capture, using either an exter-

1   nal or internal trigger. In the latter case the module self-triggers to capture only waveforms with  
 2   an amplitude greater than a specified threshold. In ProtoDUNE-SP the photon readout is con-  
 3   figured to read waveforms when triggered by a beam event, and/or to provide header information  
 4   when self-triggered by cosmic muons. The header portion summarizes pulse amplitude, integrated  
 5   charge, and time-stamp information of events. The SSP for ProtoDUNE-SP uses Gb Ethernet  
 6   communication implemented over an optical interface. The 1 Gb/s Ethernet supports full TCP/IP  
 7   protocol.

8   The module includes a separate 12-bit high-voltage DAC for each channel to provide bias to each  
 9   SiPM<sup>14</sup>. The SSP provides a trigger output signal from internal discriminators in firmware based  
 10   on programmable coincidence logic, with a standard ST fiber interface to the central trigger board  
 11   (CTB). Input signals are provided to CTB from the beam instrumentation, the SSPs, and the  
 12   beam TOF system. The CTB receives timing information from the ProtoDUNE-SP timing system  
 13   and the CTB trigger inputs are distributed to the experiment via the timing system. To that end,  
 14   the SSP implements the timing receiver/transmitter endpoint hardware to receive trigger inputs  
 15   and clock signals from the timing system.

### 16   **1.3.6.3 Electronics Next Steps**

17   Although the requirements for the electronics system are not all fully established, it is not expected  
 18   that the system will require novel high-risk techniques and can be developed and fabricated well  
 19   within the schedule for the PDS. In the latter half of CY18, ProtoDUNE-SP test beam and  
 20   cosmic-ray muon data analysis will provide evaluation of the readout system implemented in  
 21   ProtoDUNE-SP and the PD Photon Sensor and Simulation groups will provide essential guid-  
 22   ance on optimization of performance and cost.

23   As identified in Section 1.3.5, the most important near term R&D program will be to optimize the  
sec:fdsp-pd-ps  
 24   ganging scheme including choice of SiPM and cable types. The first objective is to demonstrate  
 25   that an ensemble of 48–72 Hamamatsu 6 mm × 6 mm MPPCs can be summed into a single channel  
 26   by a combination of passive and active ganging. This board will also measure the photoelectron  
 27   collection efficiency when the SiPMs are coated with TPB as a reference for ARAPUCA measure-  
 28   ments with a similar ganging level (the summing board is the same size as the ProtoDUNE-SP  
 29   ARAPUCA backplane to facilitate the comparisons). Charge processing requires a charge pream-  
 30   plifier ideally located within the cold environment, so the design must take into consideration the  
 31   failure risks and the power dissipated into the environment.

32   The timing resolution, minimum threshold and dynamic range requirements for the system are dic-  
 33   tated by the physics requirements. These are well known for the higher energy physics (>200 MeV)  
 34   but, as noted elsewhere in this document, are still evolving for lower energy. Currently, a tim-  
 35   ing resolution of 1 μs is called for and the sampling rate and number of sample bits is estimated  
 36   based on this. For this task some digital process such as a sample interpolation may be proposed,  
 37   enhancing the recorded raw sample time precision. The light sensitivity and the dynamic range  
 38   requirement will determine the number of bits and the sample rate required by either waveform or

---

<sup>14</sup>Currently there are two DAC options: one with a voltage range of 0–30 V, used with the sensL SiPMs (17 of the 24 SSP units); and the other with a range 0–60 V for use with the Hamamatsu MPPCs (7 of the 24 SSP units).

1 charge collection methods. In both cases, the signal to noise ratio and the power consumption must  
 2 be estimated. With this data from ProtoDUNE-SP and the ganging studies, the choice between  
 3 waveform readout and integrated charge readout will be made taking into account DAQ readout  
 4 and trigger requirements.

## 5 **1.4 Production and Assembly**

### 6 **1.4.1 Photon Collector Production**

7 In this section we will first describe the production process specific to each of the three Photon  
 8 Collector technologies, followed by the final assembly procedures common to all types.

#### 9 **1.4.1.1 ARAPUCA**

10 Although the individual cell dimensions may differ, the basic design of the ARAPUCA-based  
 11 PD modules for the first SP module will be similar to that of the two prototypes produced for  
 12 ProtoDUNE-SP. Here we describe the production and assembly envisaged based on that experi-  
 13 ence.

14 Each ProtoDUNE-SP ARAPUCA module is shaped as a bar with external dimensions of 207.3 cm ×  
 15 9.6 cm × 1.46 cm, which allows for it to be inserted between the wire planes through 10 slots the  
 16 APA. The module currently contains sixteen basic ARAPUCA cells, each one with an optical  
 17 window with an area of 7.8 cm × 9.8 cm and internal dimensions of approximately 8 cm × 10 cm  
 18 × 0.6 cm. The SiPMs are mounted on the backplane of the cell, which in ProtoDUNE-SP, allows  
 19 for two different configurations of either 12 or 6 passively-ganged SiPMs.

20 The internal surface of the box is lined with a dielectric mirror foil<sup>15</sup> laser cut with openings at the  
 21 locations of the SiPMs; these are visible in Figure 1.14, which shows an ARAPUCA during assembly  
 22 prior to installation of the optical windows. The backplane SiPM boards for the ProtoDUNE-SP  
 23 modules were designed at CSU and produced by an external vendor<sup>16</sup>; the SiPMs were soldered on  
 24 the boards using a reflow oven at CSU. Before mounting into the ARAPUCA module they were  
 25 tested at room and LN2 temperatures. It is anticipated that the production of the boards for SP  
 26 modules will move to Brazil.

27 want to specify Brazil?

28 The optical window of each box is a dichroic filter with cut-off at 400 nm. While the filters used for  
 29 the ProtoDUNE-SP prototypes have been acquired from Omega Optical Inc.<sup>17</sup>, other vendors are

<sup>15</sup>3M Vikuiti™ ESR - <http://multimedia.3m.com/mws/media/193294O/vikuiti-tm-esr-application-guidelines.pdf>

<sup>16</sup>Advanced Circuits Inc.; [www.4pcb.com](http://www.4pcb.com).

<sup>17</sup><http://www.omegafilters.com/>

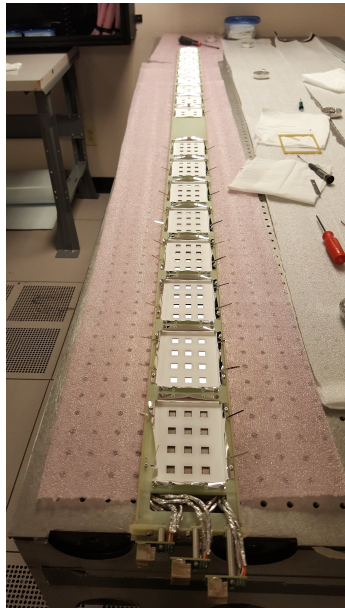


Figure 1.14: ProtoDUNE-SP ARAPUCA modules during assembly prior to installation of the dichroic filters; SiPMs and TPB coated reflector are visible.

fig:arap

1 being considered for the DUNE production<sup>18</sup>. Prior to coating, the filters are cleaned according  
 2 to the procedures given by the manufacturer using isopropyl alcohol. Since the most likely vector  
 3 for scratching/damaging the coating is dragging contaminated wipes across the surface, new clean  
 4 lint free wipes are used for each cleaning pass on the surface. Clean filters are then baked at 100°C  
 5 for 12 hours. The Vikuiti™ foils do not need to be cleaned and baked since they have a protective  
 6 film that is removed just before the evaporation.

7 The filters are coated on the external side facing the LAr active volume with pTP, while the  
 8 internal dielectric mirror side is coated with TPB. The coatings for the ProtoDUNE-SP modules  
 9 have been made at the Thin Film facility at Fermilab using a vacuum evaporator. Each coated filter  
 10 was dipped in LN2 to check the stability of the evaporated coating at cryogenic temperature. For  
 11 ProtoDUNE-SP PD production the evaporation process will be performed at UNICAMP in Brazil,  
 12 where a large vacuum evaporator with an internal diameter of one meter is now available. The  
 13 conversion efficiency of the film deposited on the filters or on the Vikuiti™ foils will be measured  
 14 with a dedicated set-up that will use the 128 nm light produced by a VUV monochromator.

### 15 1.4.1.2 Dip-Coated Light Guides

cod-bar1  
 16 To produce the full-size ProtoDUNE-SP dip-coated light guide bars, the production methods  
 17 initially developed at MIT for 20" dip-coated light guide bars were scaled up for a facility at  
 18 FNAL. For ProtoDUNE-SP production four steps will remain essentially the same:

- 19 1. Cut and polished UVT acrylic bars are annealed at 180°F in a temperature-controlled oven  
 20 to prevent subsequent crazing.

<sup>18</sup>ASHAI -Japan, Andover-USA, Edmunds Optics-USA

- 1    2. The TPB-based coating mixture is prepared in a fume hood and poured into an upright  
2    vessel located inside a larger enclosed volume.
- 3    3. A mechanized system dips the annealed bars into the coating solution where they soak and  
4    are then hung to dry in a low humidity environment established through a dry nitrogen purge  
5    of the enclosed volume.
- 6    4. The coated acrylic bars are placed in a dark box and their attenuation length in air is  
7    measured with a UV LED that is scanned along the length of the bar.
- 8    The coating solution consists of four components in the following ratios: 100 mL 99.9% pure  
9    toluene; 25 mL 200 proof ethanol; 0.2 g UVT acrylic pellets; 0.2 g scintillation grade TPB. The  
10   TPB and UVT acrylic pellets are first dissolved in a flask filled with toluene and mixed overnight  
11   with a teflon-coated magnetic stir bar. Then the ethanol is mixed into the coating solution before  
12   it is poured into the dipping vessel. This will produce an optically transparent, TPB-embedded  
13   coating, which adheres well to the surface of the bar and has a smooth surface.
- 14   A picture of the oven used for annealing, the fume hood used for mixing the coating, the vessel  
15   used for dipping, and the dark box used for measuring attenuation lengths for the production  
16   of dip-coated light guides for ProtoDUNE-SP is shown in Figure 1.15. These same production  
17   methods will also be used for the SP modules, although they will need to be scaled up so that  
18   multiple bars can be dipped and scanned at the same time. Additionally, multiple production sites  
19   will be built to produce dip-coated light guide bars for the SP modules.

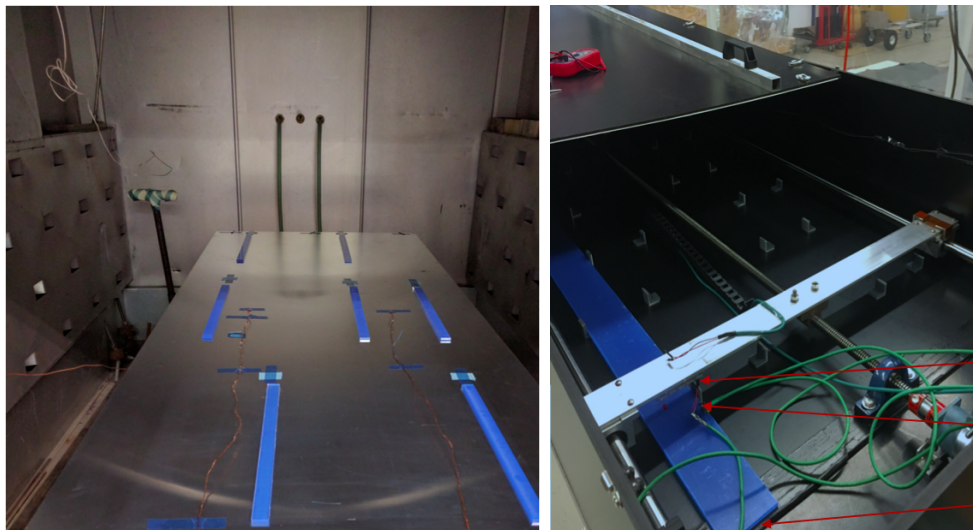


Figure 1.15: ProtoDUNE-SP dip-coated light guide bars production: annealing oven (left); dark box (right)

fig:dipp

#### 20    1.4.1.3 Double-Shift Light Guides

- 21   The production and assembly of the double-shift light guide modules has two main components; the  
22   wavelength-shifting plates and the EJ-280 light guides. Many of the production, quality assurance,

- <sup>1</sup> and assembly procedures developed for the double-shift light guide design deployed at ProtoDUNE-  
<sup>2</sup> SP will remain the same for the SP modules.

<sup>3</sup> **WLS Plates** Sheets of 1/16"-thick UVT acrylic purchased from McMaster-Carr<sup>19</sup> are laser-cut  
<sup>4</sup> into 77 cm×9 cm templates with two 34.2 cm×8.6 cm plates per template (Figure 1.16 (top)). Each  
<sup>5</sup> template also includes three small 3.81 cm×2.54 cm pop-out tabs on either side of and between  
<sup>6</sup> the two plates. After the acrylic templates are coated with TPB these tabs are separated from  
<sup>7</sup> the plate and tested in a VUV monochromator to determine the quality of the coating on the two  
<sup>8</sup> associated plates.



Figure 1.16: A laser-cut acrylic template holding two plates and three test tabs (top). TPB-coated acrylic plates after spraying during fabrication of parts for ProtoDUNE-SP (bottom).

<sup>9</sup> Scintillation grade ( $\geq 99\%$ ) TPB is dissolved in dichloromethane (DCM) at a ratio of 5 g TPB per  
<sup>10</sup> 1000 g DCM. The solution is applied to the templates using a high-volume low-pressure (HVLP)  
<sup>11</sup> sprayer system under a fume hood. The relatively small number of plates manufactured for  
<sup>12</sup> ProtoDUNE-SP were sprayed by a technician to approximate an established standard coating thick-  
<sup>13</sup> ness measured to have an acceptably high VUV photon conversion efficiency. Figure 1.16(bottom)  
<sup>14</sup> shows the HVLP spray-coating mount with a coated acrylic template. Two plates and three test  
<sup>15</sup> tabs can be seen in the HVLP mounting frame. A second sprayed template has been broken at  
<sup>16</sup> one of the midpoint cuts and positioned in the photo. For ProtoDUNE-SP production, the spray-  
<sup>17</sup> coating process will be automated or commercialized to accommodate the large-scale production  
<sup>18</sup> necessary for the SP modules.

<sup>19</sup> After spraying, the acrylic templates are baked in a vacuum oven at 80°C overnight, just below  
<sup>20</sup> the glass transition point of acrylic. The softened acrylic partially absorbs the TPB into the  
<sup>21</sup> surface, better affixing the wavelength-shifting coating. Uneven heating during the baking process  
<sup>22</sup> described above can deform the coated plates, but this is minimized by careful oven fixturing to  
<sup>23</sup> ensure even heating. After baking, the dimensions of the samples are measured and only plates  
<sup>24</sup> within the production tolerance are accepted for further testing. To ensure adequate and uniform

<sup>19</sup><https://www.mcmaster.com>

1 performance of the coated plates, the conversion efficiency is tested using a VUV monochromator.  
 2 During ProtoDUNE-SP production, plates were fabricated and tested using a McPherson<sup>20</sup> VUV  
 3 monochromator with deuterium lamp source to study performance at 128 nm. The full plates were  
 4 too large for the sample chamber VUV monochromator system, so the testing tabs on either side  
 5 of each plate were used to constrain the plate’s performance. Only plates that exhibit a relative  
 6 efficiency above an acceptance threshold are shipped to the assembly facility for deployment along  
 7 a light guide. For ProtoDUNE-SP, a threshold was chosen to accept plates that were comparable  
 8 or superior to those studied at the Blanche test stand [?] described previously.

bib:DoubleShiftLG-NIM-171113

9 **WLS-Doped Light Guides** The EJ-280 light guides are fabricated and cut to length by Eljen  
 10 Technologies. Upon receipt, each light guide is unpacked, visually inspected for defects, checked  
 11 for dimensional tolerance, and scanned using a 430 nm LED to determine its attenuation length in  
 12 air (Figure 1.17). Since the index of refraction for  $\sim$ 500 nm light in LAr is larger than in air and  
 13 the critical angle for trapping by total internal reflection is correspondingly lower, so attenuation  
 14 scans of sample light guides were made in both air and LAr (using a movable Am-241  $\alpha$  source)  
 15 to quantify the correlation between measurements in air and in LAr. Attenuation lengths longer  
 16 than  $\sim$ 5 meters measured in the darkbox correspond to attenuation lengths in LAr longer than  
 17  $\sim$ 2 meters. An acceptance threshold of 5 meters measured at both ends of an EJ-280 light guide  
 18 in the darkbox ensures adequate attenuation performance for the modules deployed in the SP  
 19 modules.

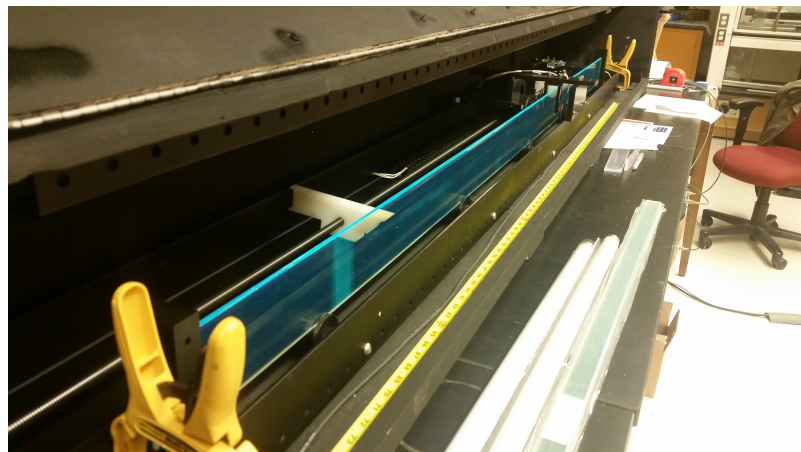


Figure 1.17: EJ-280 light guide in a dark box for attenuation scan QA at Indiana University (prepared for ProtoDUNE-SP).

20 Visual inspection of light guides received for ProtoDUNE-SP found multiple instances of fogging  
 21 or mottling on the surface and within the bulk of some light guides. However, these features did  
 22 not appear to impact the attenuation properties or uniformity during darkbox scans. Acceptance  
 23 of light guides for shipment to the assembly facility was based on the metrology and attenuation  
 24 results.

fig:pds-

<sup>20</sup><http://mcphersoninc.com>

## **1.4.2 Photon Detector Module Assembly**

Final assembly planning for PD modules is guided by the assembly of 60 ProtoDUNE-SP PD modules (representing multiple units of all three varieties) at the Colorado State University assembly facility. ProtoDUNE-SP assembly will occur at one or more assembly facilities, (number and location to be determined prior to the TDR). Several features of this are common to all three types of module, and these aspects will be covered in this section.

## **1.4.3 Incoming Materials Control**

All materials for PD module assembly will be delivered with a previously generated QC traveller (in the case of materials custom fabricated for DUNE) or will have an incoming materials traveller generated immediately upon receipt of the component (for commercial components). These travelers will be scanned upon receipt at the assembly facility, and the data stored in the DUNE QC database. Materials will either arrive with a pre-existing DUNE inventory control batch/lot number, or will have one assigned prior to entering the assembly area. Bar code labels attached to storage containers for all components in the assembly area will facilitate traceability throughout the assembly process.

Immediately upon receipt all materials will undergo an incoming materials inspection, including confirmation of key dimensional tolerances as specified on the incoming materials documentation for that component. The results of these inspections will be included on the traveller for that batch/lot and entered into the database.

In the case of discrepancy, the deviation from nominal will be recorded in an exception section of the traveller, as well as the resolution of the discrepancy.

## **1.4.4 Assembly Area Requirements**

Assembly will occur in a class 100,000 or better clean assembly area. Photosensitive components (TPB coated surfaces) are sensitive to near-UV light exposure, and will be protected by blue-filtered light in the assembly area (>400 nm or better filters<sup>21</sup>); it has been determined that this level of filtering is sufficient to protect coated surfaces during exposures of up to several days. For exposures of weeks or months, such as in the ProtoDUNE cryostat assembly area, a higher cut-off yellow filter is used<sup>22</sup>. The requirement for light exposure is to be revisited prior to ProtoDUNE-SP production.

Exposure of photosensitive components will be strictly controlled. Work flow will be restricted to ensure no component exceeds a total exposure of 8 hours to filtered assembly area lighting (including testing time).

<sup>21</sup>For example, GAMTUBE T1510 from GAM Products, Inc. - <http://www.gamonline.com/catalog/gamtube/index.php>

<sup>22</sup>F007-010 Amber with Adhesive - [http://www.epakelectronics.com/uv\\_filter\\_materials\\_flexible.htm](http://www.epakelectronics.com/uv_filter_materials_flexible.htm).

## **1 1.4.5 Component Cleaning**

<sup>2</sup> All components will be cleaned as appropriate, following manufacturer’s specifications and DUNE  
<sup>3</sup> materials test stand recommendations. Cleaning procedures will be written for all incoming ma-  
<sup>4</sup> terials, and completion of these procedures noted in the appropriate travelers.

## **5 1.4.6 Assembly Procedures**

<sup>6</sup> Following the example of the ProtoDUNE-SP experience, detailed, step-by-step written procedure  
<sup>7</sup> documents will be followed for each module, and a QC traveller for each module is completed  
<sup>8</sup> and recorded in the database. ProtoDUNE-SP experience suggests that a two-person assembly  
<sup>9</sup> team is necessary and sufficient for all three currently-considered versions of the light collector  
<sup>10</sup> modules. Our current assembly plan envisions two 2-person teams operating at the same time,  
<sup>11</sup> with a fifth person acting as shift leader. The shift leader is not directly involved in assembly,  
<sup>12</sup> but rather acts as a QC officer responsible primarily for ensuring distributing materials to the  
<sup>13</sup> assembly teams (documenting the batch/lot numbers for each detector on the relevant module  
<sup>14</sup> travelers) and ensuring that documented assembly procedures are followed.

<sup>15</sup> Assembly fixtures mounted to 2.4 m long flat optical tables will be used to support and align PD  
<sup>16</sup> components during assembly. All workers handling PD components will wear gloves, hair nets,  
<sup>17</sup> shoe covers, and clean room disposable lab jackets at all times.

## **18 1.4.7 Post-Assembly Quality Control**

<sup>19</sup> Post-assembly QC planning is currently based on ProtoDUNE-SP experience, modified as appro-  
<sup>20</sup> priate for larger-scale production. Each module will go through a series of go-no gauges designed  
<sup>21</sup> to control tolerances of critical interface points. Following this, each module will be inserted into  
<sup>22</sup> a test APA support model, representing the tightest slot allowed by APA mechanical tolerances.  
<sup>23</sup> Next, each module will be scanned at a fixed set of positions (to be determined prior to the TDR)  
<sup>24</sup> with 275 nm UV LEDs. The detector response at each position will be read out using PD readout  
<sup>25</sup> electronics, and the data compared to pre-established criteria. Figure 1.18 is a photograph of the  
<sup>26</sup> scanner used for ProtoDUNE-SP modules. These performance data will serve as a baseline for the  
<sup>27</sup> module, and will be compared against those taken in an identical scanner shortly before installa-  
<sup>28</sup> tion into the APA, as in the ProtoDUNE-SP experience. All data collected will be recorded to the  
<sup>29</sup> module traveler and to the DUNE QC database. As a final QC check, post-assembly immersion  
<sup>30</sup> into a LN2 cryostat followed by a repeat scan of each PD module (as in ProtoDUNE-SP) is being  
<sup>31</sup> considered.



Figure 1.18: PD module scanner.

fig:pds-scanner

## 1.4.8 APA Frame Mounting Structure and Module Securing

PD modules are inserted into the APA frames through ten slots (five on each side of the APA frame) and are supported inside the frame by stainless steel guide channels. The slot dimensions for the ProtoDUNE-SP APA frames were  $108.0\text{ mm} \times 19.2\text{ mm}$  wide (see Figure 1.19(top))<sup>23</sup>. The guide channels are pre-positioned into the APA frame prior to applying the wire shielding mesh to the APA frames, and are not accessible following wire wrapping. Following insertion, the PD modules are fixed in place in the APA frame using two stainless steel captive screws, as shown in Figure 1.19(bottom).

### 1.4.8.1 Cryogenic thermal contraction

Bar-style PD modules are structurally composed of primarily polycarbonate, polystyrene and acrylic, which have significantly different shrinkage factors compared to the stainless steel APA and PD support frames (see Table 1.4).

Table 1.4: Shrinkage of PD module materials for a  $206^\circ\text{C}$  temperature drop

Material	Shrinkage Factor (m/m)
Stainless Steel (304)	$2.7 \times 10^{-3}$
FR-4 G-10 (In-plane)	$2.1 \times 10^{-3}$
Polystyrene (Average)	$1.5 \times 10^{-2}$
Acrylic and Polycarbonate (Average)	$1.4 \times 10^{-2}$

<sup>23</sup>These dimensions are expected to increase by about 20% in the next round of APA design revisions, allowing for larger PD modules.

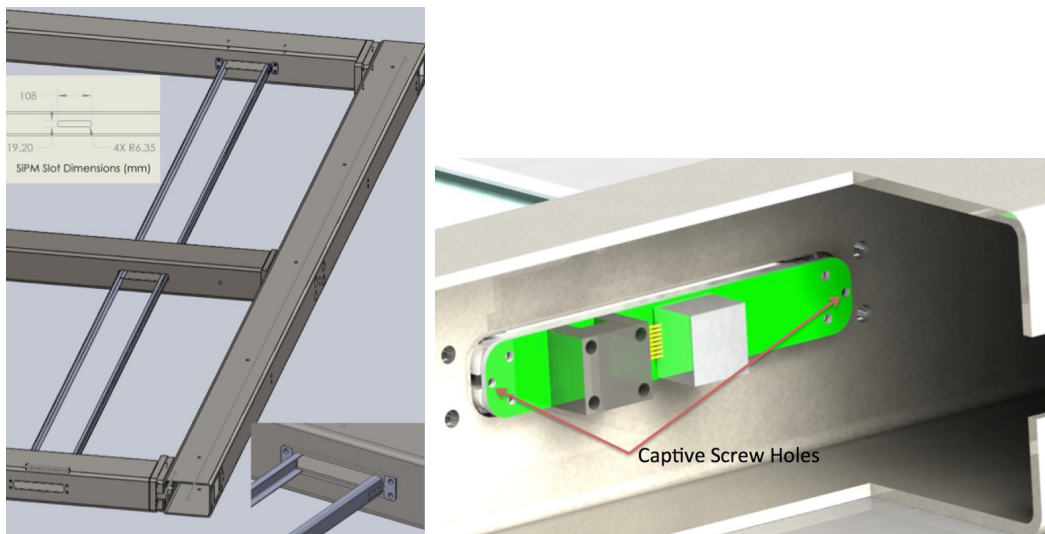


Figure 1.19: PD mounting in APA frame: Rails (top) and securing to the frame with captive screws (bottom).

fig:pds-

- <sup>1</sup> These differences in thermal expansion (or contraction, in this case) are an important factor during design of the PD module supports. Mitigation of these contractions is detailed in Table 1.5.
- <sup>2</sup> ~~tbl:fdspdshrinkeffe~~
- <sup>3</sup> Thermal expansion coefficients for the fused-silica filter plates ( $1.1 \times 10^{-4}$  m/m for a 206°C temperature drop) informed the materials selection for the ProtoDUNE ARAPUCA modules. The frame components for the ARAPUCA were fabricated from FR-4 G-10, resulting in a shrinkage of the stainless steel frame structure relative to the frame of approximately 1.2 mm along the long ( $\sim 2$  m) axis of the bar. The shrinkage of the frame relative to the filter plate is  $< 0.2$  mm. Both these relative shrinkage factors are accounted for in the dimensions and tolerances of the design.

Table 1.5: Relative Shrinkage of PD components and APA frame, and mitigations

Interface	Relative shrinkage	Mitigation
PD Length to APA width	PD shrinks 25.7 mm relative to APA frame	PD affixed only at one end of APA frame, free to contract at other end
Width of PD in APA Slot	PD shrinks 1.2 mm relative to slot width	PD not constrained in C-channels. C channels and tolerances designed to contain module across thermal contraction range
Width of SiPM mount board ( <i>Hover board</i> ) to stainless steel frame	Stainless frame shrinks 0.06 mm more than PCB	Diameter of shoulder screws and FR-4 board clearance holes selected to allow for motion
Width of SiPM mount board relative to polycarbonate mount block	Polycarbonate block shrinks 1 mm more than PCB	Allowed for in clearance holes in SiPM mount board

effects

### 1.4.8.2 PD Mount frame deformation under static PD load

FEA modeling of the PD support structure was conducted to study static deflection prior to building prototypes. Modeling was conducted in both the vertical orientation (APA upright, as installed in cryostat) and also horizontal orientation. Basic assumptions used were fully-supported fixed end conditions for the rails, with uniform loading of 3X PD mass (5 kg) along rails. Figure 1.20 illustrates the rail deflection for the APA in the horizontal (left) and vertical (right) orientations.

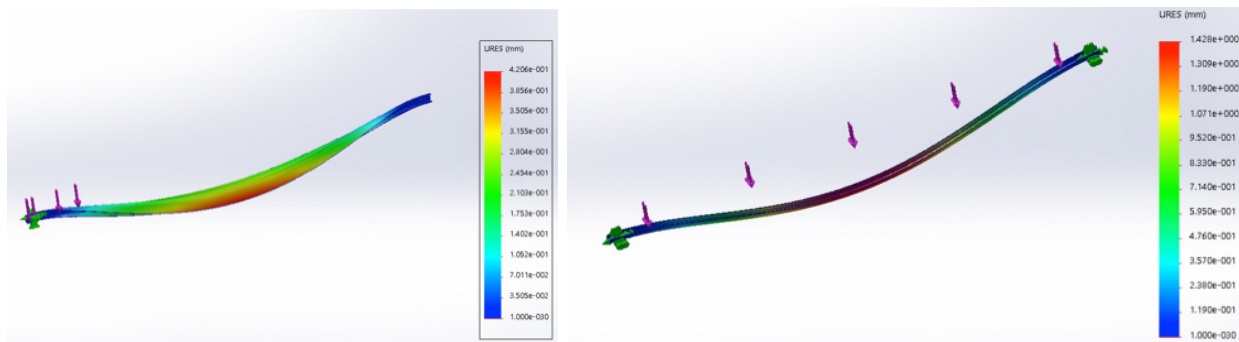


Figure 1.20: PD mechanical support analysis: Rail deflection for the APA in the horizontal (left) and vertical (right) orientations.

fig:pds-rail

### 1.4.9 Photosensor Modules

Depending on the photon collector technology selected, the SiPM analog signal will be ganged in groups of 6-48 in close proximity to the sensors inside the LAr volume; both *passive* and *active* ganging schemes are under consideration. Passive ganging (sensors in parallel) implemented with traces on the SiPM mounting board (module) and has been implemented for ProtoDUNE-SP. The SiPMs are mounted using a pick-and-place machine and standard surface mount device soldering procedures. The ganged analog signals are then brought out via long cables (approximately 25 m) for digitization outside the cryostat. ProtoDUNE-SP will provide essential operational experience with a passive ganging board and signal transport provided by Teflon ethernet CAT6 cables. It is already apparent that R&D is needed to optimize the connectors used to couple the cable to the board; it is a priority to understand the mechanical stresses involved in the SiPM-PCB-Connector system (with different CTEs) as it is cooled (or cycled) to cryogenic temperatures.

A basic level of active ganging locates summing circuitry on the board carrying the photosensors or on a separate PCB also mounted on the PD module. A more complex scheme is being considered that would include cold amplifiers and ADCs. This solution would provide more flexibility in the level of photosensor ganging and also obviate the need for carrying analog signals of long cables. Production of the board would follow standards practices but the complexity introduces concerns with reliability and long-term stability issues related to cold electronics. Basic active ganging prototypes are under study with high priority but the design is not yet at a mature stage.

## **1.4.10 Electronics**

Extensive experience of manufacturing processes was gained during the development of the SSPs under current use on ProtoDUNE-SP, a general description of the readout system of ProtoDUNE-SP can be seen in the section 1.3.6. Compatibility between elements designed by different institutions is guaranteed when standard procedures are followed so the circuit design must be done in accordance with mutually agreed-upon specification documents. A sufficient number of units needs to be produced to allow local testing and for testing in the central facility – for example, in ProtoDUNE-SP 5 12-channel SSPs were produced and delivered to CERN for integration testing prior. Twenty-four were fabricated for ProtoDUNE-SP operation.

The readout electronics of the photon detection system will be designed and produced with similar tools and protocols used for ProtoDUNE-SP. For example: printed circuit board (PCB) layout is performed in accordance with IPC specifications. Bare PCB manufacturing requirements are embedded within the Gerber file fabrication documents (e.g., layers, spacing, impedance, finish, testing, etc.). Components are assembled on to circuit boards using either trained PD consortium technical staff or by external assembly vendors, based upon volume, in accordance with per-design assembly specification documents. Testing occurs at labs and universities within the collaboration in accordance with a per-design test procedure that typically includes a mix of manual, semi-automatic and automated testing in an engineering test bench followed by overall characterization in a system- or subsystem-test stand. Other considerations and practices relevant to readout electronics production and assembly are itemized here:

- Components: Schematic capture is done using appropriate tools (such as OrCAD 16.6.<sup>24</sup> or similar toolset) available within design facility. Design is hierarchical with common front-end page referenced multiple times to ensure that all input channels are identical. The schematic contains complete bill-of-materials (BOM) including all mechanical parts. Sub-version repository is typically used for version control and backup. Multiple internal design reviews held before schematic is released to layout. The bill of materials is stored directly within schematic, extracted to spreadsheet when ordering parts. Every part is specified by both manufacturer and distributor information. Distributor information may be overridden by a technician at order time due to price and/or availability. Standard search engines such as Octopart<sup>25</sup>, ECIA<sup>26</sup> and PartMiner<sup>27</sup> are used to check price/availability across all standard distributors. A parts availability check review is performed prior to handoff from schematic to layout; as required obsolete or long lead time parts were removed from design and replaced. BOM information will include dielectric, tolerance, temperature coefficient, voltage rating and size (footprint) to ensure all parts are fully described.
- Boards: There are standard tools (such as the Allegro<sup>28</sup> toolset) available for the printed-circuit-board (PCB) layout. Conventional PCBs are realized as multi-layer, controlled impedance board with many sets of delay-matched nets. In usual practice the complete impedance and

<sup>24</sup>OrCAD™ schematic design tool for PCB design <http://www.orcad.com>

<sup>25</sup>Octopart <https://octopart.com/>

<sup>26</sup> ECIA <https://www.eciaauthorized.com>

<sup>27</sup>PartMiner <https://www.part-miner.com/>

<sup>28</sup>Cadence Allegro®PCB design solution <https://www.cadence.com>

delay characteristics are calculated within layout tool and crosschecked by PCB vendor prior to manufacture. In usual practice, a competitive bid between multiple previously qualified vendors is used, with a full electrical and impedance testing required. Multiple internal design reviews are held prior to release of the design.

- Cable plant: Cabling will be designed taking into consideration the APA space and in close collaboration with the TPC electronics group to avoid cross-talk effects. A final decision on cable procurement will be taken based on the possibility of cable manufacturing in an institution belonging to the photon detection consortium and the cost of a commercial solution.
- Manufacturer list: In addition to the general laboratory procedures for quality assurance, the general practice will be to use only printed circuit board manufacturers and external assembly vendors whose workmanship and facilities have been personally inspected by experienced production team members. All external assemblers are required to quote in accordance with an Assembly Specification document describing the IPC class and specific solder chemistry requirements of the design. The Bill of Materials document will show selected and alternate suppliers for every component of the front-end boards.
- Front-end electronics firmware: This will be specified and updated iteratively in collaboration with other systems. The electronics working group will be responsible for responding to requests for additional firmware development, including for example, modifications to timing interface, modifications to trigger interface, and implemented sensitivity to in-spill vs. not-in-spill conditions. Documents describing firmware architecture for each major change will be written and distributed to PD and DAQ working groups before implementation. Front-End electronics User's manual containing all details of new firmware will be distributed with production units when manufactured.
- Mechanical assembly: With the mechanical assembly of electronics readout boards it is common practice to use AutoCAD<sup>29</sup> with Allegro (as PCB layout tool). All relevant dimensions of the PC board including connector and indicator placement is extracted from Allegro as base DXF file from which overall exploded mechanical diagram of chassis and other mechanical parts is made. Mechanical items such as shield plates will be provided as well. It is assumed that the front-end chassis will be made by external vendors (one for chassis, one for front/back panels) from AutoCAD drawings provided by the consortium.

## 1.5 System Interfaces

This section describes the interface between the SP module PDS and several other consortia, task forces (TF) and subsystems listed below:

- APA,
- Feedthroughs,

<sup>29</sup>AutoDESK AutoCAD® computer aided design software application <https://www.autodesk.com/>

- <sup>1</sup> • TPC Cold Electronics (CE),
- <sup>2</sup> • CPA / HV System – if the coated-reflector foils option is implemented,
- <sup>3</sup> • DAQ,
- <sup>4</sup> • Calibration / Monitoring.

<sup>5</sup> The contents of the section are focused on what is needed to complete the design, fabrication,  
<sup>6</sup> installation of the related subsystems, and are organized by the elements of the scope of each  
<sup>7</sup> subsystem at the interface between them.

### <sup>8</sup> 1.5.1 Anode Plane Assembly

<sup>9</sup> The PD is integrated in the APA frame to form a single unit for the detection of both ionization  
<sup>10</sup> charge and scintillation light.

<sup>11</sup>

<sup>12</sup> **Hardware:** The hardware interface between APA and PDS is both mechanical and electrical:

- <sup>13</sup> • Mechanical: a) supports for the PDS detectors; b) access slots for installation of the detectors;  
<sup>14</sup> c) access slots for the cabling of the PD detectors; d) routing of the PDS cables inside the  
<sup>15</sup> side beams of the APA frame.
- <sup>16</sup> • Electrical: grounding scheme and electrical insulation, to be defined together with the CE  
<sup>17</sup> consortium, given the CE strict requirements on noise.

### <sup>18</sup> 1.5.2 Feedthroughs

<sup>19</sup> Several PD SiPM signals are summed together into a single readout channel. A long multi-  
<sup>20</sup> conductor cable with four twisted pairs read out the PD module. Analog signals from the SiPMs  
<sup>21</sup> are transmitted directly by cables to the appropriate flanges to outside the cryostat. All cold  
<sup>22</sup> cables originating from the inside the cryostat connect to the outside warm electronics through  
<sup>23</sup> PCB board feedthroughs installed in the signal flanges that are distributed along the cryostat roof.

<sup>24</sup> All technical specifications for the feedthroughs should be provided by the photon detector group.

### <sup>25</sup> 1.5.3 TPC Cold Electronics

<sup>1</sup> **Hardware:** The hardware interfaces between the CE and PD occur in the chimneys and the  
<sup>2</sup> racks mounted on the top of the cryostat which house low and high voltage power supplies for PD,

3 low and bias voltage power supplies for CE, as well as equipment for the Slow Control and Cryogenic  
 4 Instrumentation (SC in the following), and possibly DAQ consortia. There should be no electrical  
 5 contact between the PDS and CE components except for sharing a common reference voltage  
 6 point (ground) at the chimneys. An additional indirect hardware interface takes place inside the  
 7 cryostat where the CE and PD components are both installed on the APA (responsibility of the  
 8 single phase far detector APA consortium, APA in the following), with cables for CE and PD that  
 9 may be physically located in the same space in the APA frame, and where the cables and fibers for  
 10 CE and PD may share the same trays on the top of the cryostat (these trays are the responsibility  
 11 of the facility and the installation of cables and fibers will follow procedures to be agreed upon  
 12 in consultation with the underground installation team, Underground Installation Team (UIT) in  
 13 the following).

14 **Chimneys:** In the current design CE and PD use separate flanges for the cold/warm transition  
 15 and each consortium is responsible for the design, procurement, testing, and installation, of their  
 16 flange on the chimney, together with the LBN facility that is responsible for the design of the  
 17 cryostat. Racks on top of the cryostat: the installation of the racks on top of the cryostat is  
 18 a responsibility of the facility, but the exact arrangement of the various crates inside the racks  
 19 will be reached after common agreement between the CE, PD, SC, and possibly DAQ consortia.  
 20 The PD and CE consortia will retain all responsibilities for the selection, procurement, testing,  
 21 and installation of their respective racks, unless for space and cost considerations an agreement is  
 22 reached where common crates are used to house low voltage or high/bias voltage modules for both  
 23 PDS and CE. Even if both CE and PD plan to use floating power supplies, the consequences of  
 24 such a choice on possible cross-talk between the systems needs to be studied.

25 **Test-stands and integration facilities:** various test stands and integration facilities will be  
 26 developed. In all cases the CE and PD consortia will be responsible for the procurement, instal-  
 27 lation, and initial commissioning of their respective hardware in these common test stands. The  
 28 main purpose of these test stands is study the possibility that one system may induce noise on  
 29 the other, and the measures to be taken to minimize this cross-talk. For these purposes, it is  
 30 desirable to repeat noise measurements whenever new, modified detector components are available  
 31 for one or the other consortium. This requires that the CE and PD consortia agree on a common  
 32 set of tests to be performed and that the CE consortium can operate the PDS detectors within  
 33 a pre-determined range of operating parameters, and vice versa, without the need of providing  
 34 personnel from the PDS consortium when the CE consortium is performing tests or vice versa.  
 35 Procedures should be set in place to decide the time allocation to tests of the components of one  
 36 or the other consortium.

### 37 1.5.4 Cathode Plane Assembly and High Voltage System

38 This section describes the interface between the light collection boosting system of the SP-PDS  
 39 and the HV system. These systems interact in the case that the photon detection system includes  
 1 wavelength-shifting reflector foils mounted on the cathode plane array (CPA). The interface with  
 2 the monitoring system is addressed in Section 1.5.6.

3 **Hardware:** The purpose of installing the wavelength-shifting (WLS) foils is to allow enhanced

4 detection of light from events near to the cathode plane of the detector. The WLS foils consist of a  
5 wavelength shifting material (such as TPB) coated on a reflective backing material. The foils would  
6 be mounted on the surface of the CPA in order to enhance light collection from events occurring  
7 nearer to the CPA, and thus greatly enhancing the spatial uniformity of the light collection system  
8 as detected at the APA mounted light sensors. The foils may be laminated on top of the resistive  
9 Kapton surface of the CPA frames, with the option of using metal fasteners or tacks that would  
10 also serve to define the field lines.

11 Production of the FR4+resistive Kapton CPA frames are the responsibility of the HV consortium.  
12 Production and TPB coating of the WLS foils will be the responsibility of the Photon Detection  
13 consortium. The fixing procedure for applying the WLS foils onto the CPA frames and any required  
14 hardware will be the responsibility of the Photon Detection consortium, with the understanding  
15 that all designs and procedures will be pre-approved by the HV consortium.

16 This new detector component is not being tested in ProtoDUNE-SP, however its integration in the  
17 present SP module HV system could imply performance and stability degradation (due for example  
18 to ion accumulation at the CPA surface); the assembly procedure of the CPA/FC module could  
19 become more complex due to the presence of delicate WLS foils. Intense R&D will be required  
20 before deciding on its implementation.

21 **Integration:** An integration test stand will likely be employed to verify the proper operation of  
22 the CPA panels with the addition of WLS foils under high voltage conditions. Light performance  
23 (wavelength conversion and reflectivity efficiency) will also be verified. The HV consortium will  
24 be responsible for HV aspects of the test stand and the PD consortium will be responsible for the  
25 light performance aspects.

### 26 1.5.5 Data Acquisition

27 This section describes the PD interfaces and related requirements with the DAQ system described  
28 in Section ???. Here we list the main system interface areas.

29 **Data Physical Links:** Data are passed from the PD to the DAQ on optical links conforming to  
30 an IEEE Ethernet standard. The links run from the PD readout system on the cryostat to the  
31 DAQ system in the Central Utilities Cavern (central utility cavern (CUC)).

32 **Data Format:** Data are encoded using a data format based on UDP/IP. The data format is  
33 derived from the one used by the Dual Phase TPC readout. Details will be finalized by the time  
34 of the DAQ TDR.

35 **Data Timing:** The data shall contain enough information to identify the time at which it was  
36 taken.

1 **Trigger Information:** The PD may provide summary information useful for data selection. If  
2 present, this will be passed to the DAQ on the same physical links as the remaining data.

3 **Timing and Synchronization:** Clock and synchronization messages will be propagated from  
4 the DAQ to the PD using a backwards compatible development of the ProtoDUNE-SP Timing  
5 System protocol (DUNE docdb-1651). There will be at least one timing fiber available for each  
6 data links coming from the PDS. Power-on initialization and Start of Run setup: The PDS may  
7 require initialization and setup on power-on and start of run. Power on initialization should not  
8 require communication with the DAQ. Start run/stop run and synchronization signals such as  
9 accelerator spill information will be passed by the timing system interface.

10 **Interaction with other groups:** Related interface documents describe the interface between  
11 the CE and LBNF, DAQ and LBNF, DAQ and Photon and both DAQ and CE with Technical  
12 Coordination. The cryostat penetrations including through-pipes, flanges, warm interface crates  
13 and feedthroughs and associated power and cooling are described in the LBNF/PDS interface doc-  
14 ument. The rack, computers, space in the CUC and associated power and cooling are described in  
15 the LBNF/DAQ interface document. Any cables associated with photon system data or commu-  
16 nications are described in the DAQ/Photon interface document. Any cable trays or conduits to  
17 hold the DAQ/CE cables are described in the LBNF/Technical Coordination interface documents  
18 and currently assumed to be the responsibility of Technical Coordination.

19 **Integration:** Various integration facilities are likely to be employed, including vertical slice tests  
20 stands, PDS test stands, DAQ test stands and system integration/assembly sites. The DAQ  
21 consortia will provide hardware and software for a vertical slice test. The PD consortium will  
22 provide PD emulators and PD readout hardware for DAQ test stands. (The PD emulator and PD  
23 readout hardware may be the same physical object with different configuration). Responsibility  
24 for supply and installation of DAQ/PD cables in these tests will be defined by the time of the  
25 DAQ TDR.

## 26 **1.5.6 Calibration and Monitoring**

27 This subsection concentrates on the description of the interface between the SP-PD and Cali-  
28 bration/Monitoring Task Force (CTF), since there are components of the system planned to be  
29 installed with the HV system Cathode, and through field cage (FC) strips and FC ground plane  
30 (GP).

31 **Hardware:** The SP-PD has proposed the photon-detector gain and timing calibration system to  
32 be also used for SP-PD monitoring purposes during commissioning and experimental operation. A  
33 pulsed UV-light system is proposed to cross-calibrate and monitor the DUNE-SP photon detectors.  
34 The hardware consists of warm and cold components.

35 By placing light sources and diffusers on the cathode planes designed to illuminate the anode planes  
36 the photon detectors embedded in the anode planes can be illuminated. Cold component (diffusers  
37 and fibers) interface with High-Voltage and will be described in a separate interface document.  
38 Warm components include controlled pulsed-UV source and warm optics. These warm components  
1 will interface CTF with Slow-Controls/DAQ subsystems and will be described in corresponding  
2 documents. Optical feedthrough is a cryostat interface.

3 Hardware components will be designed and fabricated by SP-PDS. Other aspects of hardware  
4 interfaces are described in the following. The CTF and PDS groups might share rack spaces that  
5 needs to be coordinated between both groups. There will not be dedicated ports for all calibration  
6 devices. Therefore, multi-purpose ports are planned to be shared between various groups. CTF  
7 and SP-PD will define ports for deployment. It is possible that SP-PD might use Detector Support  
8 Structure (DSS) ports or TPC signal ports for routing fibers. The CTF in coordination with other  
9 groups will provide a scheme for interlock mechanism of operating various calibration devices (e.g.  
10 laser, radioactive sources) that will not be damaging to the PD.

11 The PD has proposed the photon-detector gain and timing calibration system. The system will be  
12 used for PD monitoring purposes during commissioning and for standard experimental operation.  
13 A pulsed UV-light system is proposed to cross-calibrate and monitor the DUNE-SP photon detec-  
14 tors. The hardware consists of warm and cold components. By placing light sources with diffusers  
15 on the cathode planes, the system is designed to illuminate the photon detectors embedded in  
16 the anode planes. The details are described in the DUNE Interface Document: SP-PDS/CTF.  
17 Cold components of the calibration system (diffusers and fibers) interface with the HV system.  
18 Diffusers are installed at CPA, and therefore reside at the same CPA potential. Quartz fibers are  
19 insulators used to transport light from optical feedthroughs (at the cryostat top) through FC GP,  
20 and through FC strips to the CPA top frame. These fibers are then optically connected to diffusers  
21 located at CPA panels. Required fiber resistance is defined by HV system requirements to ensure  
22 the cathode is protected from shorting out due to fiber conductivity. PD hardware components  
23 will be designed and fabricated by PD.

## 24 **1.6 Installation, Integration and Commissioning**

### 25 **1.6.1 Transport and Handling**

26 Following assembly and testing of the PD modules they will be carefully packaged and shipped to  
27 the FD site for checkout and any final testing prior to installation into the cryostat. Handling and  
28 shipping procedures will depend on the environmental requirements determined for the photon  
29 detectors, and will be specified prior to the TDR.

30 A testing plan will be developed to determine environmental requirements for photon detector  
31 handling and shipping. The environmental conditions apply for both surface and underground  
32 transport, storage and handling. Requirements for light (UV filtered areas), temperature, and  
33 humidity exposure will also be developed.

34 Handling procedures that ensure environmental requirements are met will be developed. This will  
35 include handling at all stages of component and system production and assembly, testing, shipping,  
36 and storage. It is likely that PD modules and components will be stored for periods of time during  
1 production and prior to installation into the FD cryostats. Appropriate storage facilities need to  
2 be constructed at locations where storage will take place. Shipping and storage containers need to  
3 be designed and produced. Given the large number of photon detector modules to be installed in

- 4 the FD, it will be cost effective to take advantage of reusable shipping containers.
- 5 Documentation and tracking of all components and PD modules will be required during the full  
6 production and installation schedule. Well defined procedures will be in place to ensure that all  
7 components/modules are tested and examined prior to, and after, shipping. Information coming  
8 from such testing and examinations will be stored in a hardware database.
- 9 An Integration and Test Facility (ITF) will be constructed at a location to be decided by the  
10 collaboration/project for the integration of the PDs into anode plane assemblies. Transportation  
11 to and from ITF should be carefully planned. The PDS units will be shipped from the production  
12 area in quantities compatible with the APA transport rates.
- 13 Operations: The PDS deliveries will be stored in temperature and humidity controlled storage  
14 area. Their mechanical status will be inspected.
- 15 Transportation to SURF: The delivery to SURF will be such that the storage time before integra-  
16 tion will be at most two weeks.

## 17 **1.6.2 Integration with APA and Installation**

1-pd-apa

18 PD modules integration into the APA frame will happen at the Integration facility. Experts from  
19 both groups will work with the installation team. An electrical test with APA/PDS/CE will be  
20 performed at the integration facility in a cold box, after the integration of PDS and CE on the  
21 APA frame has been completed.

22 The APA consortium will be responsible for the transportation of the integrated APA frames  
23 from the integration facility to the LBNF/SURF facility. The UIT team, under supervision of the  
24 APA group, will be responsible to move the equipment into the clean room. Work on the 2-APA  
25 connection and inspection underground, prior to installation in the cryostat, is performed by the  
26 APA group. Work on cabling during this assembly process is performed by PDS and CE groups  
27 under supervision of the APA group. Once the anode plane assemblies will be moved inside the  
28 cryostat, the PDS and CE consortia will be responsible for the routing of the cables in the trays  
29 hanging from the top of the cryostat.

## 30 **1.6.3 Installation into the Cryostat and Cabling**

-pd-cryo

31 The PD modules are installed into the anode plane assemblies. There are ten PD's per APA,  
32 inserted into alternating sides of the APA frame, five from each direction. Once a PD is inserted,  
33 it is attached mechanically to the APA frame and cabled up with a single power/readout cable.  
1 Following PD installation cold electronics (CE) units are installed at the top of the APA frame.

2 After the APA has been integrated with the PDS and CE, it will be moved via the rails in the  
3 clean room to the integrated cold test stand for testing and be moved into the cryostat. The two

4 anode planes of the TPC will be assembled inside the cryostat, each of the fully tested anode plane  
5 assemblies mechanically linked together. Signal cables from the TPC readout and the PD modules  
6 are routed up to the feedthrough flanges on the cryostat top side. The cables from each of the CE  
7 and PD's on the APA are then routed and connected to the final flanges on the cryostat.

#### **8 1.6.4 Commissioning: Calibration and Monitoring**

11-calib  
9 Commissioning of the SP module PDS will rely heavily on the readout electronics, DAQ, and  
10 calibration and monitoring system. Deployment and testing of the readout electronics separately  
11 from the in situ installation of photon detector modules in the APA is important to establish their  
12 proper functioning before connection to the photon detectors or their flanges. Careful checking  
13 at each step of the integration process will help to find unexpected problems early enough to be  
14 corrected before individual units are mounted into the larger systems (first in the APA then after  
15 installation in the cryostat).

16 Once the electronics are readout out via the DAQ system, it will be appropriate to add the PD  
17 modules and continue commissioning of the installed system. In order to be properly tested the PD  
18 modules will have to be in the dark. Making sure it is possible to make this check frequently enough  
19 to catch problems early is critical. This will have to be balanced with the needs of installation, as  
20 work progresses.

21 Once the basic operation of the readout system is established, the calibration and monitoring  
22 system will be of great use during the commissioning. While the background signals from the  
23 warm photon detectors may make calibration difficult, the monitoring system will be able to  
24 flash UV light to excite the PD modules. These light signals can be used to determine that  
25 cabling is connected, and connected properly by looking at light from different UV emitters. Once  
26 the detector is beginning to cool down, the operation of the calibration and monitoring system  
27 will become even more important as the monitoring of the individual channels should be a good  
28 indication of their proper operation, and again, the proper cabling and interface.

## **29 1.7 Quality Assurance and Quality Control**

### **30 1.7.1 Design Quality Assurance**

31 PD design quality assurance (QA) focuses on ensuring that the detector modules meet the following  
32 goals:

- 1 • Physics goals as specified in the DUNE requirements document,
- 2 • Interfaces with other detector subsystems as specified by the subsystem interface documents,

- 3     • Materials selection and testing to ensure non-contamination of the LAr volume.
- 4     The PDS consortium will perform the design and fabrication of the components in accordance  
5     with the applicable requirements of the LBNF/DUNE Quality Assurance Plan. If the institute  
6     (working under the supervision of the consortium) performing the work has a documented QA  
7     program the work may be performed in accordance with their own program.
- 8     Upon completion of the PDS design and QA/quality control (QC) plan there will be a prelim-  
9     inary design review process, with the reviewers charged to ensure that the design demonstrates  
10    compliance with the goals above.

## 11    **1.7.2 Production and Assembly QA**

12    The photon detector system will undergo a QA review for all components prior to completion of  
13    the design and development phase of the project. The ProtoDUNE-SP test will represent the most  
14    significant test of near-final PD components in a near-DUNE configuration, but additional tests  
15    will also be performed. The QA plan will include, but not be limited to, the following areas:

- 16     • Materials certification (in the FNAL materials test stand and other facilities) to ensure  
17        materials compliance with cleanliness requirements
  - 18     • Cryogenic testing of all materials to be immersed in LAr, to ensure satisfactory performance  
19        through repeated and long-term exposure to LAr. Special attention will be paid to cryogenic  
20        behavior of plastic materials (such as radiators and light guides), SiPMs, cables and connec-  
21        tors. Testing will be conducted both on small-scale test assemblies (such as the small test  
22        cryostat at CSU) and full-scale prototypes (such as the full-scale CDDF cryostat at CSU).
  - 23     • Mechanical interface testing, beginning with simple mechanical go-nogo gauge tests, followed  
24        by installation into the ProtoDUNE-SP system, and finally full-scale interface testing of the  
25        PDS into the final pre-production TPC system models
  - 26     • Full-system readout tests of the PD readout electronics, including trigger generation and  
27        timing, including tests for electrical interference between the TPC and PD signals.
- 28    Prior to the release of the TDR the PDS will undergo a final design review, where these and other  
29    QA tests will be reviewed and the system declared ready to move to the pre-production phase.

## 1    **1.7.3 Production and Assembly Quality Control**

2    Prior to the start of fabrication, a Manufacturing/QC Plan will be developed detailing the key  
3    manufacturing, inspection and test steps. The fabrication, inspection and testing of the compo-  
4    nents will be performed in accordance with documented procedures. This work will be documented  
5    on travelers and applicable test or inspection reports. Records of the fabrication, inspection and

6 testing will be maintained. When a component has been identified as being in noncompliance to  
7 the design, the nonconforming condition shall be documented, evaluated and dispositioned as use-  
8 as-is (does not meet design but can meet functionality as is), rework (bring into compliance with  
9 design), repair (will be brought into meeting functionality but will not meet design) and scrap.  
10 For products with a disposition of accept as is or repair, the nonconformance documentation shall  
11 be submitted to the design authority for approval.

12 All QC data (from assembly and pre- and post-installation into the APA) will be directly stored  
13 to the DUNE database for ready access of all QC data. Monthly summaries of key performance  
14 metrics (TBD) will be generated and inspected to check for quality trends.

15 Based on the ProtoDUNE-SP model, we expect to conduct the following production testing:

- 16 • Dimensional checks of critical components and completed assemblies to insure satisfactory  
17 system interfaces.
- 18 • Post-assembly cryogenic checkouts of SiPM mounting PCBs (prior to assembly into PD  
19 modules).
- 20 • Cryogenic testing of completed modules (in CSU CDDF or similar facility) to provide a final  
21 pre-shipping module test.
- 22 • Warm scan of complete module using motor-driven LED scanner (Or UV LED array).
- 23 • Complete visual inspection of module against a standard set of inspection points, with photo-  
24 photographic records kept for each module.
- 25 • End-to-end cable continuity and short circuit tests of assembled cables.
- 26 • Front-end electronics functionality check.

#### 27 **1.7.4 Installation Quality Control**

28 PDS pre-installation testing will follow the model established for ProtoDUNE-SP. Prior to in-  
29 stallation in the APA, the PD modules will undergo a warm scan in a scanner identical to the  
30 one at the PD module assembly facility and the results compared. In addition, the module will  
31 undergo a complete visual inspection for defects and a set of photographs of all optical surfaces  
32 taken and entered into the QC record database. Following installation into the APA and cabling  
1 an immediate check for electrical continuity to the SiPMs will be conducted.

2 It is expected that following the mounting of the TPC cold electronics and the photon detectors  
3 the entire APA will undergo a cold system test in a GAr cold box, similar to that performed  
4 during ProtoDUNE-SP. During this test, the PDS system will undergo a final integrated system  
5 check prior to installation, checking dark and LED-stimulated SiPM performance for all channels,  
6 checking for electrical interference with the cold electronics, and confirming compliance with the

7 detector grounding scheme.

## 8 1.8 Safety

1-safety  
9 Safety management practices will be critical for all phases of the photon system assembly and test-  
10 ing. Planning for safety in all phases of the project, including fabrication, testing and installation  
11 will be part of the design process. The initial safety planning for all phases will be reviewed and  
12 approved by safety experts as part of the initial design review. All component cleaning, assembly,  
13 testing and installation procedure documentation will include a section on safety concerns relevant  
14 to that procedure, and will be reviewed during the appropriate pre-production reviews.

15 Areas of particular importance to the PDS include:

- 16 • Hazardous chemicals (particularly WLS chemicals such as TPB used in radiator bar dipping  
17 and spraying) and cleaning compounds: All chemicals used will be documented at the  
18 consortium management level, with MSDS and approved handling and disposal plans in  
19 place.
- 20 • Liquid and gaseous cryogens used in module testing: Full hazard analysis plans will be  
21 in place at the consortium management level for all module or module component testing  
22 involving cryogenic hazards, and these safety plans will be reviewed in the appropriate pre-  
23 production and production reviews
- 24 • High voltage safety: Some of the candidate SiPMs require bias voltages above 50 VDC, which  
25 may be a regulated voltage as determined by specific labs and institutions. Fabrication and  
26 testing plans will demonstrate compliance with local HV safety requirements at the particular  
27 institution or lab where the testing or operation is performed, and this compliance will be  
28 reviewed as part of the standard review process.
- 29 • UV and VUV light exposure: Some QA and QC procedures used for module testing and  
30 qualification may require use of UV and/or VUV light sources, which can be hazardous  
31 to unprotected operators. Full safety plans must be in place and reviewed by consortium  
32 management prior to beginning such testing.
- 33 • Working at heights, underground: Some aspects of PDS module fabrication, testing and in-  
34 stallation may require working at heights, or deep underground. Safety considerations will be  
35 taken into consideration during design and planning for these operations, all procedures will  
1 be reviewed prior to implementation, and all applicable safety requirements at the relevant  
2 institutions will be observed at all times.

## 3 1.9 Organization

### 4 1.9.1 Single-Phase Photon Detection System Consortium Organization

5 The Photon Detection System (PDS) consortium follows the typical organizational structure of  
 6 DUNE Consortia:

- 7 • A Consortium Lead (Ettore Segreto) provides overall leadership for the effort, and attends  
 8 meetings of the Executive and Technical Boards.
- 9 • A Technical Lead (David Warner) provides technical support to the consortium lead, attends  
 10 the Technical Board and Integration/Project meetings, oversees the project schedule and  
 11 WBS, and oversees the operation of the project working groups. In the case of the PDS, the  
 12 Technical Lead is supported by a Deputy Technical Lead (Leon Mualem).

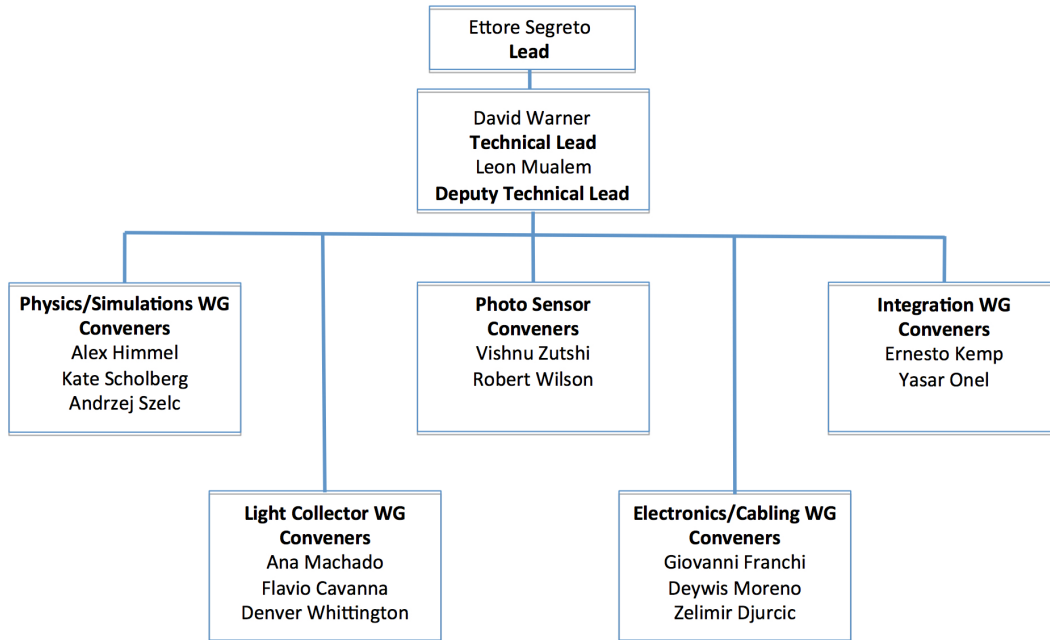


Figure 1.21: Photon Detector System consortium organization chart.

13 Below the leadership, the consortium is divided up into five working groups, each led by two or  
 14 three working group conveners as shown in the PDS Management Table of Organization. Each  
 15 working group is charged with one primary area of responsibility within the consortium, and the  
 16 conveners report directly to the technical lead regarding those responsibilities. As the consortium  
 17 advances to a more detailed WBS and project schedule, it is envisioned that each working group  
 18 will be responsible for one section of those documents.

1 The working group conveners are appointed by the PDS Project Lead and Technical Lead, and  
 2 the structure may evolve as the consortium matures and additional needs are identified.

### 3 1.9.2 Planning Assumptions

4 Plans for the PDS consortium are based on the overall schedule for DUNE. In particular the APA  
5 schedule defines the time window for the completion of the final development program on the light  
6 collectors: A final down-select to a baseline light collector option, photosensors, and front-end  
7 electronics must be made by late-February 2019. Due to the early stage of development for the  
8 ARAPUCA light collector system, we may maintain an alternate light collector option up to the  
9 pre-production review in September of 2020, but all other systems must be defined prior to the  
10 TDR.

11 For planning purposes we assume that the photon detector system modules will undergo final  
12 assembly and testing at one or more PDS assembly facilities, with an initial assembly rate of  
13 approximately twenty modules per week, accelerating to forty modules per week in the second half  
14 of module fabrication.

15 We further assume that the modules will be shipped from the fabrication facilities to a detector  
16 integration facility, at a site to be determined later, to be integrated along with the cold electronics  
17 into the APA frames and cold tested in a cryogenic test facility. We plan for an initial rate of two  
18 anode plane assemblies per week, with the possibility of accelerating to four anode plane assemblies  
19 per week as production lessons are learned. PD personnel will be present at the integration facility  
20 to oversee the installation and testing.

21 Meeting this timeline requires that the development of the ARAPUCA system be aggressively  
22 pursued throughout CY2018, with a goal of testing near-final prototypes in the late fall of 2018  
23 and allowing technology comparisons between the ARAPUCA and the light guide technologies in  
24 winter of 2019.

25 Additional development efforts prior to the TDR will focus on

- 26 • Identifying and selecting reliable cryogenic photosensor (SiPM) candidates,
- 27 • Reducing cost and optimizing performance of front-end electronics,
- 28 • Solidifying PDS performance requirements from additional physics simulation efforts.

29 We assume that apart from these items, where rapid development is still required, most of the  
30 detector components to be delivered by the PD consortium will require only minor changes rela-  
31 tive to the ProtoDUNE-SP components. For this reason the modifications of these other detector  
32 components will be delayed until 2019, which will also help with the availability of funding. Ex-  
33 ceptions will be made for further development in test stands for cabling studies, and for interface  
34 engineering required to ensure satisfactory integration of the PD with the APA and cold electronics  
35 systems.

### 1.9.3 High-Level Schedule

- The high-level schedule for the photon detector consortium through submission of the TDR at the end of Q2 in FY19 is detailed in Figure 1.22 and the pre-TDR key milestones are listed in Table 1.6.

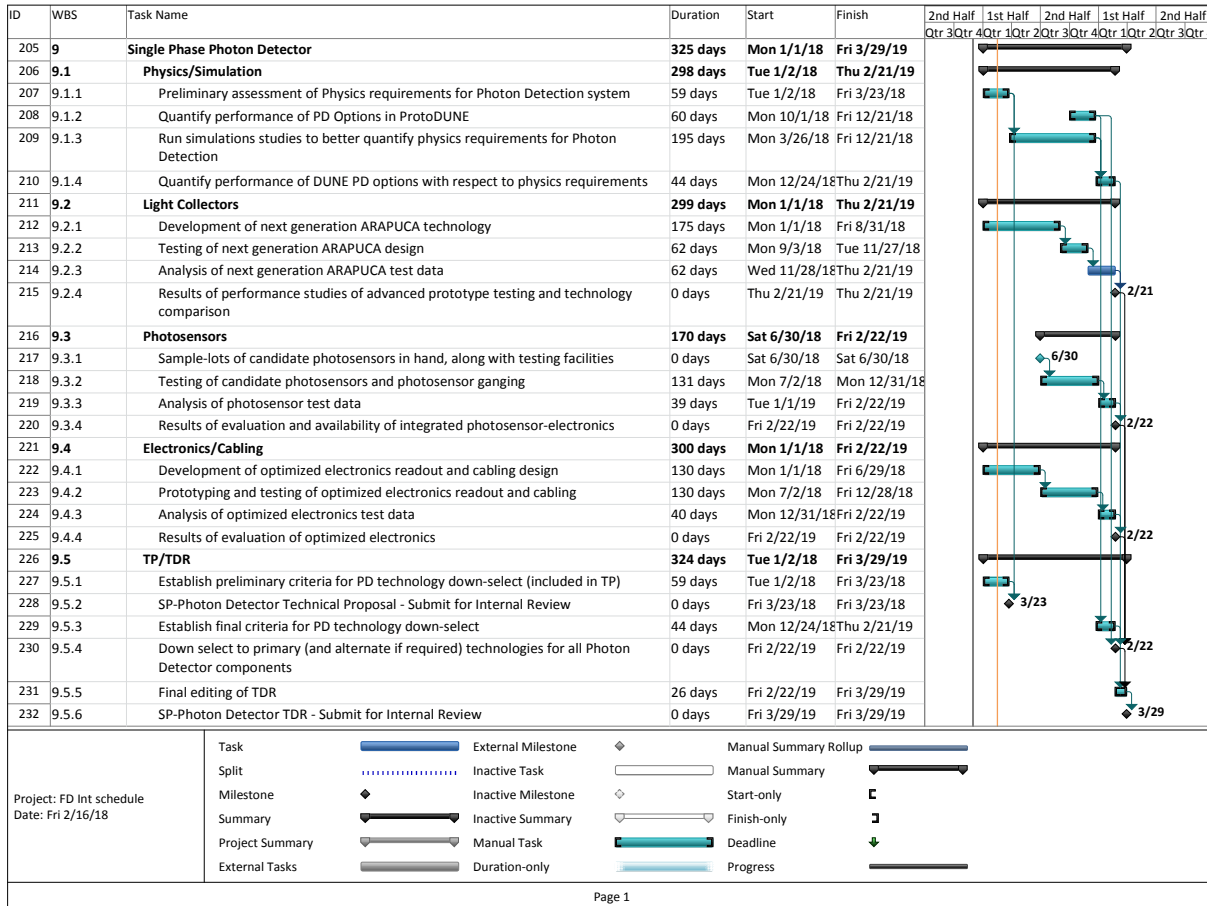


Figure 1.22: Photon Detector System consortium schedule through to the TDR.

- High-level post-TDR milestones are listed in Table 1.7.

Table 1.6: Pre-TDR Key Milestones.

Milestone	Date
Preliminary PD technology selection criteria determined	3/21/18
Results from final prototype light collector studies available	2/21/19
Final PD technology selection criteria available	2/21/19
Down-select to primary (and potential alternate) light collector technology	2/22/19
Submit initial TDR draft for internal review	3/29/19

Table 1.7: Post-TDR Key Milestones.

Milestone	Date
PD pre-production review(s) complete	3/2020
Initial PD module fabrication begins	9/2020
Final PD production review based on initial production QA	2/2021
First PD modules delivered for installation	5/2021
Installation into anode plane assemblies begins	6/2021
PD fabrication complete (first 10 kt module)	7/2023



# <sup>1</sup> References

- <sup>2</sup> [1] DOE Office of High Energy Physics, “Mission Need Statement for a Long-Baseline Neutrino  
<sup>3</sup> Experiment (LBNE),” tech. rep., DOE, 2009. LBNE-doc-6259.